SYNTHESES AND INVESTIGATION OF ELECTROCHEMICAL PROPERTIES OF SELENOPHENE AND BENZOTRIAZOLE BEARING COPOLYMERS

A THESIS SUBMITTED TO
THE GRADUATE SCHOOL OF NATURAL AND APPLIED SCIENCES
OF
MIDDLE EAST TECHNICAL UNIVERSITY

BY

HANDE ÜNAY

IN PARTIAL FULFILLMENT OF THE REQUIREMENTS
FOR
THE DEGREE OF MASTER OF SCIENCE
IN
POLYMER SCIENCE AND TECHNOLOGY

SEPTEMBER 2014

Approval of the thesis:

SYNTHESES AND INVESTIGATION OF ELECTROCHEMICAL PROPERTIES OF SELENOPHENE AND BENZOTRIAZOLE CONTAINING COPOLYMERS

submitted by **HANDE ÜNAY** in partial fulfillment of the requirements for the degree of **Master of Science in Polymer Science and Technology Department, Middle East Technical University** by,

Prof. Dr. Canan Özgen _____
Dean, Graduate School of **Natural and Applied Sciences**

Prof. Dr. Teoman Tinçer _____
Head of Department, **Polymer Science and Technology**

Assoc. Prof. Dr. Ali Çırpan _____
Supervisor, **Chemistry Dept., METU**

Assoc. Prof. Dr. H. Emrah Ünalan _____
Co-supervisor, **Metallurgical and Materials Eng. Dept., METU**

Examining Committee Members:

Prof. Dr. Levent Toppare _____
Chemistry Dept., METU

Assoc.Prof. Dr. Ali Çırpan _____
Chemistry Dept., METU

Asisst. Prof. Dr. İrem Erel Göktepe _____
Chemistry Dept., METU

Assoc. Prof. Dr. Yasemin Arslan Udum _____
Adv. Tech. Dept., Gazi Univ.

Dr. Görkem Günbaş _____
Chemistry Dept., METU

Date: 05/09/2014

I hereby declare that all information in this document has been obtained and presented in accordance with academic rules and ethical conduct. I also declare that, as required by these rules and conduct, I have fully cited and referenced all material and results that are not original to this work.

Name, Last name: Hande Ünay

Signature:

ABSTRACT

SYNTHESES AND INVESTIGATION OF ELECTROCHEMICAL PROPERTIES OF SELENOPHENE AND BENZOTRIAZOLE BEARING COPOLYMERS

Ünay, Hande

M. S., Polymer Science and Technology Department

Supervisor :Assoc.Prof. Dr. Ali Çırpan

Co-Supervisor : Assoc.Prof. Dr. Emrah Ünalan

September 2014, 76 pages

Polymers containing selenophene as a π bridge; poly(2-(2-octyldodecyl)-4-(selenophen-2-yl)-7-(5-(thiophen-2-yl)selenophen-2-yl)-2H-benzo[d][1,2,3]triazole) (**P-SBTTh**) and poly(2-(2-octyldodecyl)-4-(5-phenylselenophen-2-yl)-7-(selenophen-2-yl)-2H-benzo[d][1,2,3]triazole (**P-SBTPh**) were synthesized via Stille and Suzuki coupling, respectively. Optical and electrochemical properties were investigated and comparisons with their thiophene analogs were done. Selenophene substitution resulted in low band gap and red shifted absorption, high switching times (less than 1s) with reasonable optical contrast. Although both polymers showed moderate stability during chronoamperometry studies,**P-SBTPh** showed high stability in NIR region with fast

switching times. Switching time of **P-SBTPh** was 0.2 second that is the fastest switching time compared to all benzotriazole-based polymers.

Keywords: Selenofen, Low Band Bap, Fast Switching Time, Benzotriazole

ÖZ

SELENOFEN VE BENZOTİAZOL İÇEREN KOPOLİMERLERİN SENTEZİ VE ELEKTROKİMYASAL ÖZELLİKLERİNİN İNCELENMESİ

Ünay, Hande

Yüksek Lisans, Polimer Bilimi ve Teknolojisi Bölümü

Tez Yöneticisi : Doç.Dr. Ali Çırpan

Ortak Tez Yöneticisi : Doç.Dr. Emrah Ünalan

Eylül 2014, 76 sayfa

Bu çalışmada, π-köprüsü olarak selenofen içeren poli(2-(2-oktildodesil)-4-(selenofen-2-yl)-7-(5-(tiyofen-2-il)selenofen-2-il)-2H-benzo[d][1,2,3]triazol) (**P-SBTTh**) ve poli(2-(2-oktildodesil) -4 (5-fenilselenofen-2-il) -7 (selenofen-2-il)-2H-benzo [d] [1,2,3] triazol (**P-SBTPh**) sırasıyla Still eve Suzuki kenetlenme reaksiyonları ile sentezlenmiştir. Optik ve elektrokimyasal özellikleri incelenmiş ve tiyofen analoglarıyla bu özelliklerin karşılaştırmaları yapılmıştır. Selenofen eklenmesi düşük bant aralığına ve absopsiyonun kırmızı alana kaymasına ve kayda değer optik kontrast ile hızlı anahtarlama zamanına (1sn'den daha az) neden olmuştur. Her iki polimerde kronoamperometri çalışmalarında düşük kararlılık gösterse de, **P-SBTPh** yakın

kızılötesi alanda yüksek kararlılık ve hızlı anahtarlama zamanına sahip olduğu gözlenmiştir.**P-SBTPh** 0.2 sn anahtarlama zamanı ile benzotrizol temelli tüm polimerler içerisinde en hızlı anahtarlama zamanına sahip polimerdir.

Anahtar kelimeler: Selenofen, Düşük Bant Aralığı, Yüksek Anahtarlama Zamanı, Benzotriazol.

To my precious family

ACKNOWLEDGEMENTS

First and foremost I would like to express my sincere gratitude to my supervisor Assoc. Prof. Dr. Ali Çırpan for his endless patience, excellent support and invaluable guidance during my thesis study. I am aware of that although I graduated, he will remain as an excellent advisor for me during my life. It has been an honor for me to be his graduate student.

I am grateful to Prof. Dr. Levent Toppare for his scientific support, expertise andvaluble suggestions. I owe him gratitude for his scientific cooperation and contributions to my thesis studies.

I would like to thank you to Şerife Hacıoğlu for her elaborate electrochemistry studies.

I would like to thank you to Dr. Görkem Günbaş for his contributions to my thesis. I cannot ignore his valuble sugesstions about organic chemistry.

There are no enough words to express my gratitude to Naime Akbaşoğlu Ünlü. She became more than a lab boss from the moment I started to study in Çırpan research group. She always tried to teach me anything that she knows about organic chemistry at every opportunitiy. I am grateful to her for anything I know. Also, I would like to thank to her for endless patience and support during my thesis studies. She was alwayswith me with a shoulder to cryin my bad times. I will never forget the daysthat we stayed awake till morning with red eyes in front of the computer to write my papers. I feel so lucky for having such a lovely friend who will always support me expecting anything in return.

I would like to thank to Özlem Şener and Tuğba Şensöz for their long standing friendships, sisterhood and for being ready to listen to me timeless. I ensure you with no doubt, you will remain as a sister even years and life separate us.

I would like to express my feelings to Ece Aktaş and Cansel Temiz for their friendship, motivations and advices. I wish I had to chance to meet them before. I will never forget the coffee breaks and ‘’Kaave Falı’’.

I am grateful to have chance to knowOzan Erlik and Emre Ataoğlu. I appreciate them for their friendship, motivations and support. They always stand for me anytime I needed.

Also, I would like to thank to all Çırpan Research Group members for their friendships, motivations and providing such a peacefull and admirable working environment. All my lab memories are special for me. It has always made me feel lucky and special to being a part of Çırpan Research Group member.

There is one person I want to offer my special and endless thanks to Tamer Onat for his excellent support, understanding, being next to me in any conditions and time, and his invaluable love. I would not withstand against difficulties and injustice without his love and support. I consider myself lucky for having his perfect friendship and love.

I would like to thanks to my lovely brother Hakan Ünay with whom I opened my eyes into the world and I am still growing up. Thanks to him I never feel alone and hopeless.

Finally, words alone cannot express my gratitude to my dear family. It is great to feel your love and support always by my side.

TABLE OF CONTENTS

LIST OF TABLES

TABLES

LIST OF FIGURES

FIGURES

LIST OF SCHEMES

SCHEMES

LIST OF ABBREVATIONS

CP Conjugated Polymer

PA Polyacetylene

PT Polythiophene

P3AT Poly (3-alkyl)thiophene

PPy Polypyrolle

PEDOT Polyethylenedioxythiophene

PINT Polyisothianaphtene

PPP Poly-paraphenylene

PPS Poly-paraphenylenesulfide

PANI Polyaniline

PPV Poly-paraphenylenevinylene

HOMO Highest Occupied Molecular Orbital

LUMO Lowest Unoccupied Molecular Orbital

P-SBTTh Poly(2-(2-octyldodecyl)-4-(selenophen-2-yl)-7-(5-(thiophen-2-yl)selenophen-2-yl)-2H-benzo[d][1,2,3]triazole)

P-SBTPh Poly(2-(2-octyldodecyl)-4-(5-phenylselenophen-2-yl)-7-(selenophen-2-yl)-2H-benzo[d][1,2,3]triazole

IR Infrared

VB Valence Band

CB Conduction Bande

BLA Bond Length Alternation

D Donor

A	Acceptor
OSC	Organic Solar Cell
OLED	Organic Light Emitting Diode
ECD	Electrochromic Device
HTL	Hole Transport Layer
ETL	Electron Transport Layer
HIL	Electron Injection Layer
TCO	Transparent Conducting Oxide
PEDOT	Poly (3,4-ethylenedioxythiophene
PSS	Polystyrene sulfonate
BTz	Benzotriazole
ACN	Acetonitrile
$TBAF_6$	Tetrabutylammoniumhexafluorophosphate

CHAPTER 1

1. INTRODUCTION

1.1 Conjugated Polymers

The conducting ability of polymeric materials are emanating from their π -conjugation between their repeating units that can be clearly defined as extension and delocalization of overlapped π-electrons provide conjugated orientation [1]. Eventhough, semiconducting characteristic of π-conjugated polymershas been known since 1862, the tremendous interest of academia and industry aimed at development of new designed conjugated polymers (CPs) for organic electronics, organic photonics and biosensor has awaken in recent years [2]. The trigger of this growing interest in the field was the discovery of conducting polyacetylene in 1977 by Alan J. Heeger, Alan G. MacDiarmid and Hideki Shirakawa. Later on, the three scientists were awarded by Nobel Prize in Chemistry in 2000 for this excellent discovery.Unlike inorganic semiconductors, conjugated polymers have outstanding advantages like flexibility, low cost, corrosion resistant and processability. Additionally, optical and electronic properties of CPs can be easily altered via synthetic modification [3-5]. Owing to these advantages, CPs have become good candidate to replace inorganic semiconductors. Thanks to their fascinating electronic and optical characteristics and easily tunable morphology, CPs has given rise to enhancement in organic electronics and organic photonics areas such; photovoltaic cells [6], light emitting diodes (LEDs) [7], field effect transistors [8], electrochromics [9] and biosensors [10].

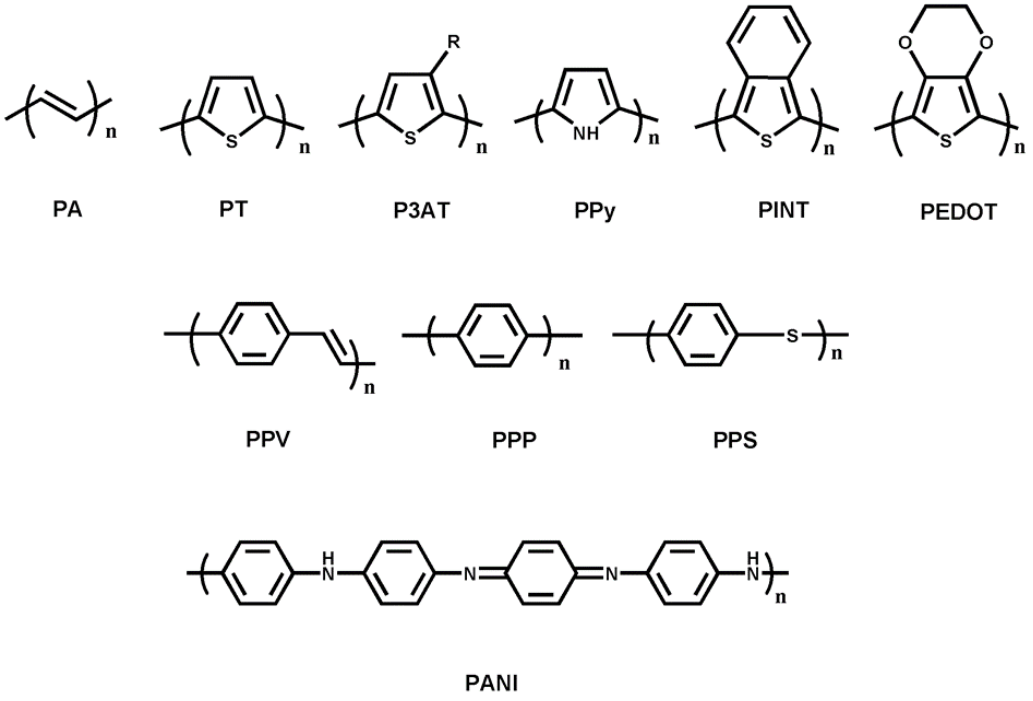

Figure 1. Some of the most widely used conjugated polymers

1.2 Brief History of Conjugated Polymers

The essential investigations on CPs which gave guidance to today's academic and industrial researches, started in 1960s at two different places in the world. In America, Alan J. Heeger andAlan G. MacDiarmid synthesized an inorganic polymer, sulfur nitride $(SN)_x$through solid-state polymerization of S_2N_2 crystals. The conductivity measurements at room temperature indicated high results as $2.5x10^3$ $S.cm^{-1}$ As the temperature was decreased to 10 K, the conductivity of the polymer was increased over hundreds orders of magnitude. Besides, when both Br_2 and I_2 were applied to inorganic polymer, 10^4 to 10^7increase in conductivity was observed [11]. This invention opened a new class of materials, conducting polymeric metals [12].

In the meantime, in Japan, polyacetylene (PA) was synthesized directly as a thin film formby mistake by Hideki Shirakawa and his coworkers [13]. The use of thousand times greater Ziegler-Natta catalyst in reaction resulted in insoluble powders. The analysis of infrared (IR) spectra of thin films demonstrated that the stereochemistry of double bonds was affected by the temperature of polymerization. It was observed that at lower temperatures the trans content of PA was diminished. Additionally, at higher temperatures (~ 145 ^{o}C) the cis form converted to trans form irreversibly as shown in **Figure2**. Electronic studies of cis-trans isomers pointed that the resistivity and energy gap of trans rich PA were $1.0x10^{4}$ Ω.cm and 0.56 eV, respectively. In comparison, cis rich PA had $2.4x10^{8}$ Ω.cm resistiviy and 0.93 eV energy gap [13].

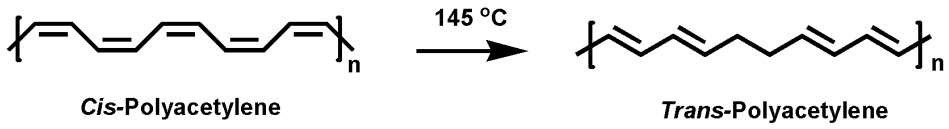

Figure 2. Irreversible isomerization of polyacetylene

At the end of 1960s Hideki Shirakawa, Alan MacDiarmid and Alan J. Heeger started collobrative studies on behaviour of PA with respect to different oxidants [13,14]. They observed different conductivity for PA through different oxidants. The highest conductivity at room temperature was obtained as 38 $S.cm^{-1}$ with treatment with I_2.

In 1977, the study of oxidatively doped trans-PA, which exhibited metallic conductivity, was reported by these two collabrative research groups [4]. This tremendous discovery is considerd as the launch of a new field, plastic electronics

alsomentioned as synthetic metals. In 2000, the three scientists were awarded with Nobel Prize in Chemistry ‘‘*for the discovery and development of conductive polymers*’’.

1.3 Band Theory

Solids are classified in three main groups with respect to separation of their occupied and unoccupied energy levels; insulators, semiconductors and conductors. In respect to band theory, the gap between valence band and conduction band of a solid assigns the conductivity. The movement of electrons from valence band (VB) to conduction band (CB) through excitation of electron photochemically or thermally causeconductivity. According to band theory, CB and VB of metals overlapped as a single band hence, the metals have zero band gap [4,15]. The metals, whichare also named as conductors, have partially filled bands, which allow movement of free charge carriers resulting in conduction. On the contrary,in insulators, the gap is separated with a large energy thereby the migration of electrons from VB to CB is impossibleto conduct electricity. Semiconductors take place in the group between insulators and conductors in terms of conductivity. [16].

The band structure of semiconductors is composed of partially filled valence and empty conduction bands.CPs which have extented π-conjugation between their repeating units, take place in the group of semiconductors. As a result of their extended π-conjugation, CPs can gain ability of conductivity via doping which is described in following sections. As a matter of fact, the π-band of a conjugated polymer is regarded as VB and π* band is also known as CB.

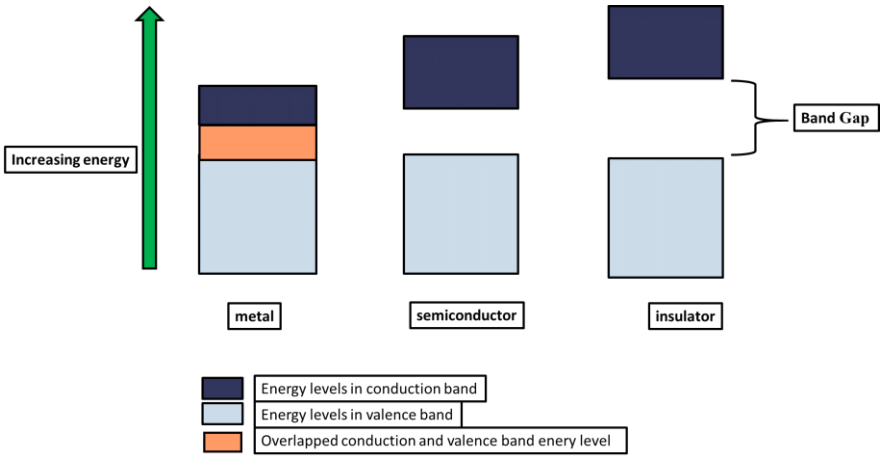

Figure 3. Band gaps of metal, semiconductor and insulator in comparison

1.4 Band gap enginering

Optical and electrochemical properties of the conjugated polymers strongly depend on band gap of the polymers. Therefore, several methodologies have been developed to control band gap and synthesize conjugated polymers with desired properties for certain applications. Bond length alternation (BLA), inductive and mesomeric effect of substituents, chemical rigidification and donor-acceptor approach are the developed strategies for this purpose [17].

Conjugated polymers have two possible resonance structures in their ground state, namely quinoid and aromatic forms. Quinoid form of the polymer is less energetic due to destruction of the aromaticity to adopt this form. Bond length alternation is defined as the ratio of aromatic to quinoid population in a conjugated system and depending on this ratio band gap can be lowered. Conjugated polymers with less aromatic units in the conjugated main chain can easily adopt the quinoid form through π-electron delocalization, which lowers the band gap [17].

Anchoring electron-donating or electron-withdrawing groups onto the aromatic unit in the main chain is another effective way to control band gap via inductive or mesomeric effects. In general, if electron-donating groups were utilized as substituent, HOMO energy level is raised, while anchoring electron-withdrawing groups lower the LUMO energy. Thus strategy lowers the band gap [17].

Controlling steric and electronic effects on main chain via molecular modification is also useful strategy for band gap engineering. Chemical rigidification is one way to decrease rotational disorder, which increases planarity between adjacent and delocalization. Thus causes decrease in BLA and band gap. Donor- acceptor theory is also another and most effective technique and explained in following section in detail [17].

1.5 Donor-acceptor approach

Alternation of electron rich (donor) and electron deficient (acceptor) units along the same backbone to control electron delocalization, quinoid structures formation and bond length alternation of the conjugated polymers, is known as donor-acceptor approach. This theory was first discovered by Havinga et al; and they showed that different combination of donor and acceptor units strongly affect the band gap of the polymer and a low band gap polymer was synthesized by proper combination of these units [18,19]. Syntheses of lower band gap conjugated polymers compared to parent components are explained by perturbation theory that explain the formation of new HOMO and LUMO energy levels from the interaction of donor and acceptor segments. Interaction of HOMO energy level of acceptor and HOMO energy level of acceptor cause formation of a new HOMO energy level, which is higher than that of parent components. Similarly, formation of the new LUMO energy level from this interaction

is lower. This causes a decrease in the band gap of polymer compared to their counterparts. Therefore, careful design and selection of the donor and acceptor moieties can provide control over optical and electronic properties. Besides, combination of different donor and acceptor units offer polymers with different band gaps. Therefore, syntheses of novel polymers require a systematic analysis on nature of donor and acceptor units [17].

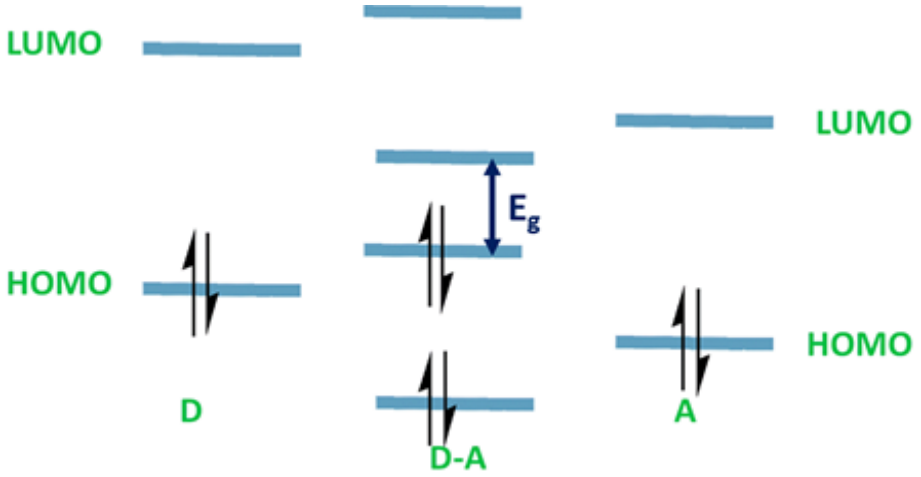

Figure 4. Effect of orbital couplings of donor-acceptor units on band gap

1.6. From π-Conjugated Polymers to Conducting Polymers: Doping Process and Doping Types

1.6.1 Doping Process

According to several parameters related to conductivity such as mobility and population density of charge carrier and charge on the electron, CPs are regarded as insulators. However, owing to their semiconductor band structure that allows electronic excitation or electron addition/elimination CPs can gain the ability of conducting. When a charge carrier is introduced to polymer backbone via oxidation or reduction,structure of the chain is distorded in a way that low energy states defined as polaron, bipolaron are formed within bandgap [2]. On account of doping, holes or electrons can move along the polymer backbone to satisfy electrical conductance. By virtue of doping process, conductivity of CPs is increased several orders of magnitude [20]. Both doping and dedoping process are irreversible processes, which do not alter the chemical structure of backbone of CPs.

1.6.2 Doping Types

The mobile charge carriers, which are holes, or electrons that move along the backbone of CPs leading to electrical conductivitiy, generally do not exist in the backbone of CPs intrinsically. In order to give conducting ability to CPs, these mobile charge carriers can be obtained through two main doping processes:

Anionic doping is also named as *''p-type doping''*can be carried out through electrochemical or chemical oxidation. When a positive potential is applied to CP, a dopant anion moves in from the solution into the CP in the direction of the delocalizedcharge sites on the CP, in this way anionic doping electrochemically arises [21]:

$$\text{trans-}[CH]_x + xyClO_4^- \longrightarrow [CH^{y+}\ ClO_4^{y-}\ ]_x + (xy)\ e^-$$

To accomplish anionic doping chemically, CP is exposed to a solution or vapor of an oxidative dopant [22,23]:

$$\text{trans-}[CH]_x + 1.5xyI_2 \longrightarrow [CH^{y+}\ I_3^{y-}]_x$$

Cathodic electrochemical or chemical reduction. Likewise, when a negative potential is applied in solution to CP immobilized on inert electrode, a dopant cation moves in from the solution into the CP in the direction of the delocalized charge sites on the CP, consequently cathodicdoping electrochemically occurs[24] :

$$\text{trans-}[CH]_x + xyLi^+ + (xy)e^- \longrightarrow [Li_y^+\ CH^{y-}]_x$$

In order to execute cathodic doping chemically, CP is exposed to a solution or vapor of a reductive dopant [21,23]:

$$\text{trans-}[CH]_x + (xy)Na^+(Nphth)^- \longrightarrow [Nay^+\ (CH)^{y-}]_x + Nphth$$

1.7 Synopsis of Polymerization Methods

Several polymerization methods can be utilized to synthesize conducting polymers. Chemical and electrochemical polymerization techniques are the most common ones

for polymerization. The chemical polymerization is generall based on Palladium (Pd) catalyzed cross coupling reactions or oxidative ferric chloride polymerization. Electrochemical polymerization involves oxidation of monomers into polymerson electrode surface via applied potential. When two techniques are compared electrochemical polymerization has advance in time sequence since polymerization occurs in seconds and also the produced polymer is oxidatively doped. On the contrary, chemical polymerization (except oxidative ferric chloride polymerization) requires several hours and synthesized polymer is need to be doped chemically or electrochemcially to their conducting form [25].

1.8 Chemical Polymerization

1.8.1 Oxidative Ferric Chloride Polymerization

In oxidative ferric chloride polymerization, monomer is polymerized through $FeCl_3$ as a reagent as shown in **Figure 5.**

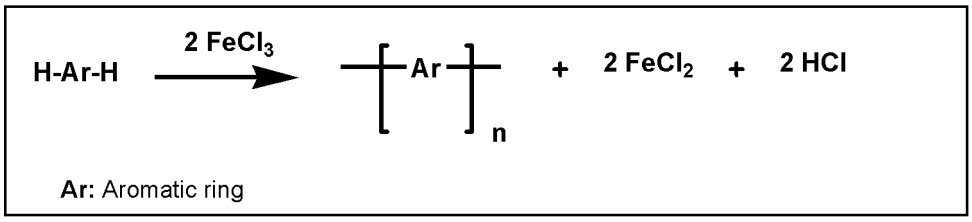

Figure 5. Oxidative ferric chloride polymerization

Oxidative polymerization takes place where the hydrogen atom is attached. As a result, it requires no active groups such as stannyl or halide. Oxidative ferric polymerization is preferrable in order to attain polymers with high molecular weights [26].

1.8.2 Palladium-Catalyzed Cross Coupling Polymerization

Palladium-catalyzed carbon-carbon bond forming reactions have been widely used in organic sytnthesis due to their relatively mild conditions and tolerance to variety of functional groups.Palladium-catalyzed cross coupling reactions as shown in **Scheme 1.**occurs in four main steps; ligand dissociation, oxidative addition of the metal, transmetalation, reductive elimination. In the first step, the catalyst ML_n, such as $Pd(PPh_3)_4$, where M stands for metal (Ni^o, Pd^o, Pt^o) and Lrepresents ligand, dissociates to create the more reactive catalyst with two phosphine groups. Hence, $Pd(PPh_3)_2$ become the active catalyst. The phosphine groups donate their lone pair to empty d orbital on Pd, resulting σ bonding within phoshine groups and Pd. In this manner, the electron density on Pd is increased hence its nucleophilicity is enhanced. As a result, the second step of the cross coupling reactions, which is oxidative addition becomes inevitable. In this step, an organo-halide (RX) is added to Pd(II) complex through oxidative addition. Transmetalation step involves transfer of nuclophile bonded to organometallic compound from metal to the Pd (II) complex. In the final step, the product is eliminated from Pd catalyst reductively, and the two ligands are transferred to Pd catalyst, therefore Pd catalyst is regenerated Pd(0) for the next cycle [27-28].

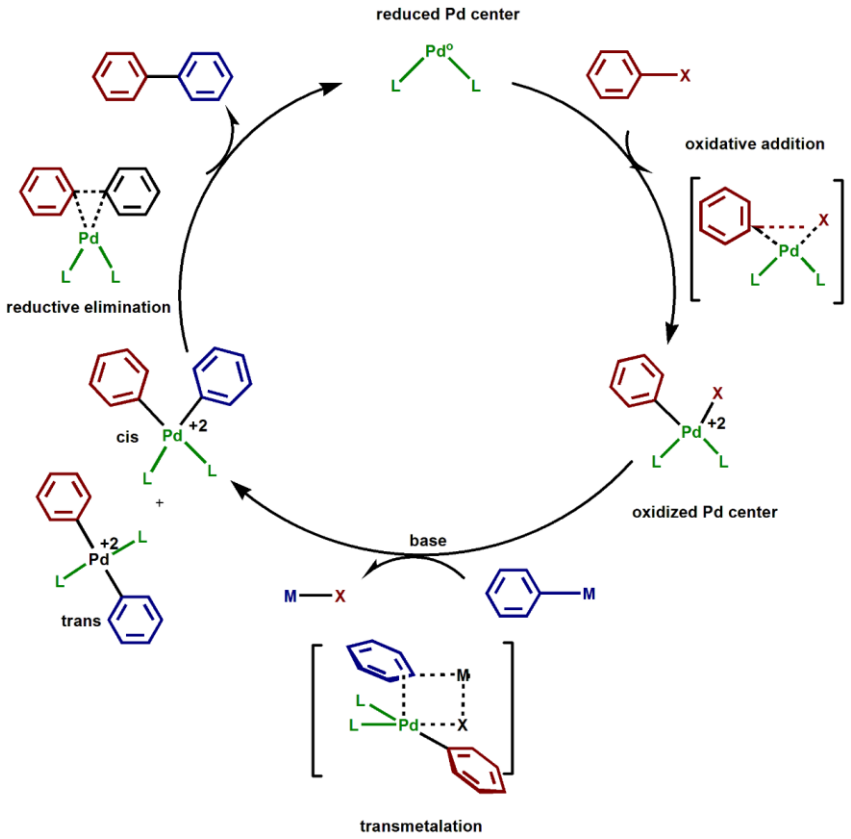

Scheme 1. Mechanism of Palladium- catalyzed cross coupling reaction

1.9 Electrochemical Polymerization

Electrochemical polymerization involves oxidation of monomers on the surface of indium tin oxide (ITO) coated glass upon applied potential. Electrochemical polymerization provides advantages for further investigations of optical and electrochemical properties of the resulted polymer since it has been already coated on electrode. However, the resulted polymers are in small amounts and also they are generally insoluble. Hence, thermal caharcterizations and molecular weight analysis of the polymers are consequently are imposibble.

Duing electropolymerization, radical cations are formed and they participate in radical coupling reactions and also electrochemical reactions resulting formation of long polymer chain. The following radical coupling and electrochemical reactions are represented as $E(CE)_n$mechanism as shown in **Scheme 2.** representing electrochemical polymerization of thiophene unit [29].

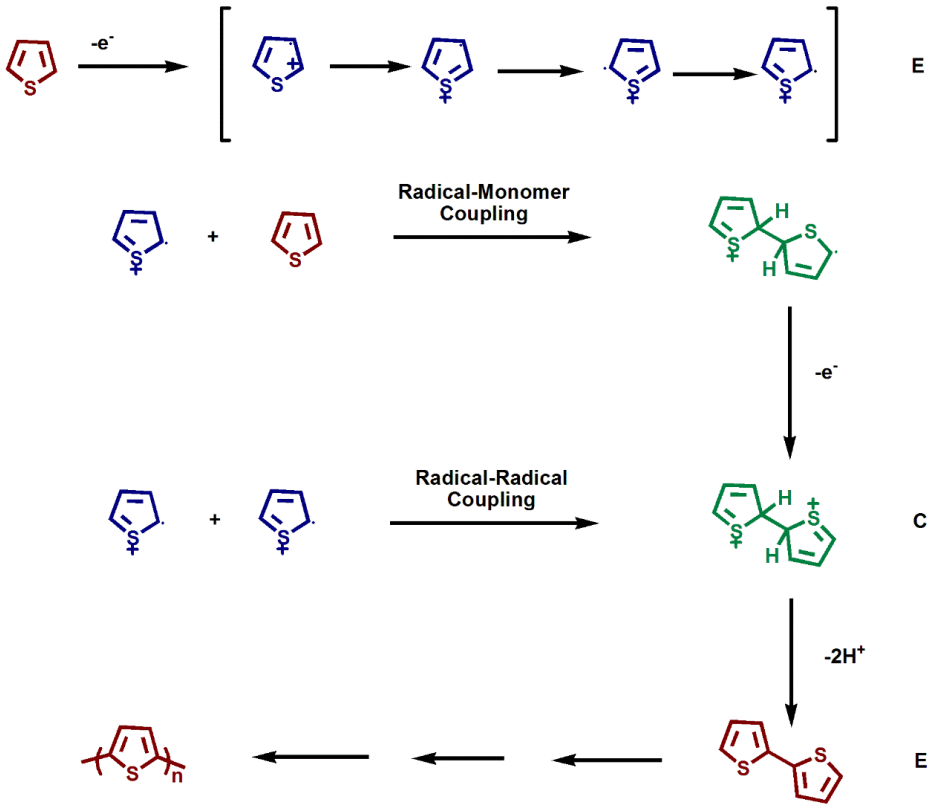

Scheme 2. Proposed mechanism of electropolymerization of thiophene

In the electrochemical step of $E(CE)_n$ mechanism, the monomer is oxidized and radical cation is formed. Electron transfer reaction occurs much faster than monomer diffusion

from bulk solution hence concentration of radical cations is high near the electrode surface. The second step, chemical reaction step includes the coupling reactions between radical cations or radical cation and monomer to for generate dimer unit in neutral form.Upon applied potential, the dimer unit undergones oxidation and forms its radical cation via coupling reactions which results a trimer unit.As polymerization progresses through following electrochemical and chemical reactions, solubility decreases dramatically and the desired polymer precipitates on the surfaceof electrode [30,31].

1.10 Electrochromism

Chromism is defined as reversible color change upon applied a chemical or physical external stimulus. Chromism is classified according to the applied stimulus resulting in color change such as thermochromism, photochromism, halochromism, solvatochromism, piezochromism and electrochromism. Electrochromism is the reversible and visible color change associated with reduction or oxidation processes caused by applied potential. Different colors are observed due to the generation of different electronic absorption bands during redox processes. The color change is commonly observed between a colored state and a transparent state, or between two colored states. In some cases, formation of several color states can take place due to formation of two redox states, which is named as multichromism [32]. Transition metal oxide, molecular dyes and conducting polymers are three classes of electrochromic materials.

1.11 Types of Electrochromic Materials

1.11.1 Transition metal oxide films

These kinds of electrochromic materials areclassified under inorganic electrochromic materials. Many transition metal oxides in the thin film form like iridium, rhodium, ruthenium, tungsten, manganese, and cobalt exhibit electrochromic property. Tungsten trioxide (WO_3) electrochromic properties were discovered in 1969. After that, it is studied widely. WO_3 is cathodically coloring material and it is transparent in its neutral state. Blue color forms when it is reduced. The accepted mechanism is the injection and extraction of electrons and metal cations like Li^+, H^+, play a crucial role on electrochromic properties of WO_3 [33].

$$WO_3 + xM^+ + xe^- \rightarrow M_xWO_3$$

(transparent) (blue)

1.11.2 Viologens

Chemical structure of viologens (1,1'-disubstituted- 4,4'-bipyridilium salts) and their redox processes are depicted in **Scheme 3.** Viologens might have two-step reduction and optical and electrochemical properties of them can be tailored by different conditions like substitution and ion selection. Different alkyl chain or substituents can be anchored to viologens and color of this material is strongly affected by

thesechanges. For example, if the substituent is *n*-heptyl, a purple color is observed whereas if p-cyano-phenyl was the substituent, a green color is observed [32].

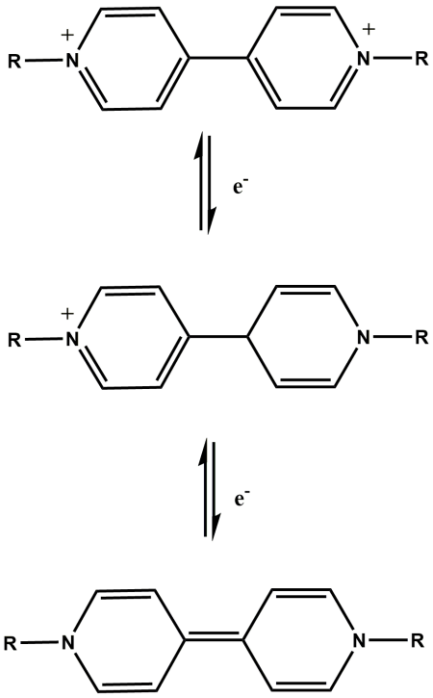

Scheme 3. Redox process of viologens

1.12 Electrochromism in Conducting Polymers

Electrochromic conjugated materials have aroused great attention in the recent years due to their advantages over inorganic counterparts. Electrochromic conjugated polymers have rapid response times, and high optical contrasts and they are more processable compared to inorganic counterparts. Furthermore, color tunability can do by structure modifications via monomer functionalization and copolymerization.

Electrochromic properties of conjugated polymers are affected by band gap which is the energy difference between valence band and conduction band. Conjugated polymers are insulators in their neutral states. Optical properties of conjugated polymers change by electrochemical or chemical doping and dedoping process. This process causes the introduction of new states (intraband transitions) in the band gap, which is responsible from optical changes and conductivity. Oxidation of conjugated polymers results in the formation of charge carriers like polarons and bipolarons. Therefore, doping process is the main reason for electrochromism in conjugated polymers. Every color of the spectrum can be attained with conjugated polymers [34]. For example, P3HT, polypyrrole and polyaniline switch between red and blue, yellow and black, yellow, green, blue, and violet respectively [35]. The color of neutral state and doped state of conjugated polymers strongly changed by band gap. For example, polymers with band gap greater than 3 eV are transparent in the neutral form and they absorb light in visible region after doping process. Whereas, polymers with band gap equal to or less than 1.5 eV absorb light in visible region and become transparent after doping process. Therefore, factors affecting band gap is the key point to synthesize novel polymers with different neutral state colors

1.13. Applications of Conducting Polymers

The discovery of conducting polymers (CP) has opened a new erawhere the CPs are regarded as *''plastic electronics''*. They have several advantages such as flexibility, processability, low cost. Additionally, they exhibit outstanding electronic and optic properties. They have been used in fabrication of electronic device, solar energy conversion [36], supercapacitors [37], electrochromic devices [38], transistors [39], light emmiting diodes [40] and biosensors [41].

1.14 Organic Light Emitting Diodes

Organic light emitting diodes (OLEDs) are solid state light sources consisting of thin film which is an electroluminescent organic material sandiwiched between an anode and a cathode. Upon applied potential, electrons and holes are introduced into the electroluminescent material. With the recombination of electrons and holes, excitons are formed which decay by fluorescence with a frequency given by the energy difference between HOMO and LUMO of the electroluminescent material. So overall, light is emitted upon applied potential. Additional thin film layer can be used to utilize hole and electron transport which are named as hole transport layer (HTL) and electron transport layer (ETL).Additionally to enhance the hole transport hole injection layer (HIL) can be introduced to device [42].

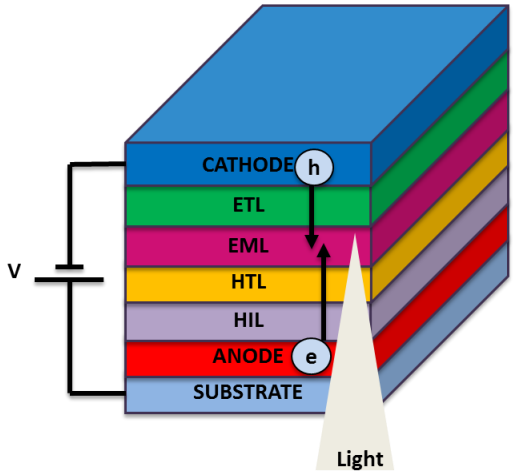

Figure 6. Organic light emitting diode device structure

1.15 Organic Solar Cells

Organic solar cells (OSCs) are photovoltaic devices that converst the light energy directly to the electrical energy. The main goal to use organic solar cells is the harvesting light energy from the sun. OSCs performs under illmunination and produce electrical current that can be directly used or stored chemically or mechanically. OSCs mainly are composed of transparent conducting oxide (TCO) as anode, hole transport layer, active layer (donor: acceptor blend) and cathode. There are five main steps for the operation of organic solar cells: 1) absorption of light by donor material in the active layer, 2) formation of electron and hole pairs which named as *''excitons''*3) diffisuon of exciton to the donor-acceptor interface 4) dissociation of exciton, 5) charge collection by the corresponding electrodes. In OSC device configuration, anode is indium tin oxide (ITO), the hole transport layer is poly (3,4-

ethylenedioxythiophene):polystyrene sulfonate (PEDOT:PSS) and the acceptor material is generally a fullerene derivative [43].

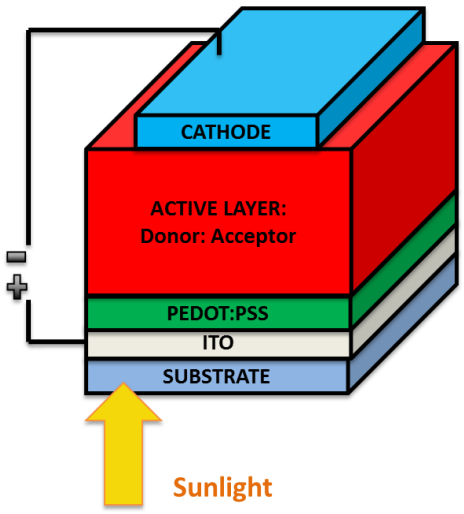

Figure 7. Schematic representative of organic solar cell device configuration

1.16 Electrochromic Devices

As it is mentioned in detail in the text electrochromism is the reversible and visible color change of the material upon applied potential. Electrochromic conjugated polymers owe good UV-vis absorption, fast switching times, high colorination efficiency and excellent optical contrast besides their color can be tuned through modification of different molecules and groups.

The absorptive/tranmissive electrochromic device works through reversible color change of electrochromic material between colored and bleached states. In this device

configuration, both counter and working electrodes are transparent in order to allow to light to pass through the electrochromic device.

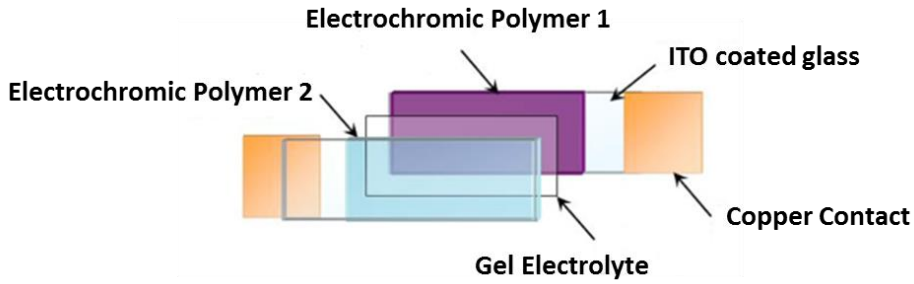

Figure 8. Schematic absorptive/ transmissive ECD

Electrochromic devices allow light and heat control through changing their light transmission properties upon applied potential.Electrochromic devices can work either reflective or transmissive mode. The reflective mode operates to decrease the reflected light such as car rear view mirrors. With this aim, one of the electrical contact is covered with a reflactive material such as mirror. In transmissive mode, all layers are transparent, for this reason both electrical contacts are chosen as transparent [44].

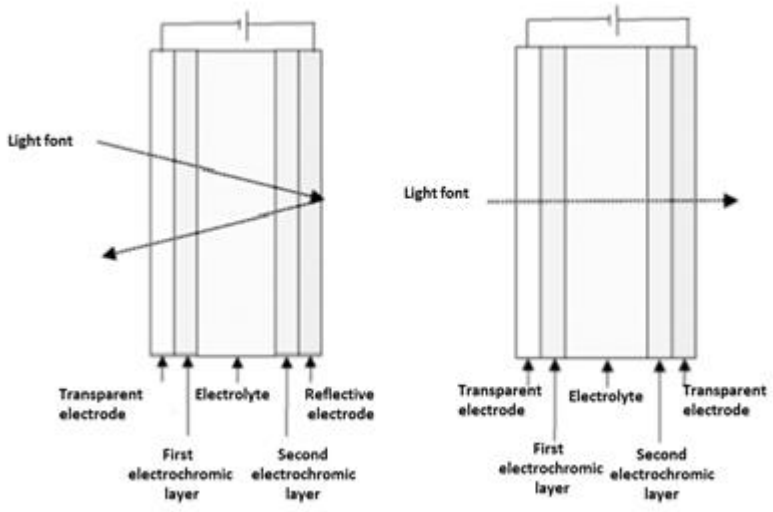

Figure 9. Shematic representative electrochromic device operating at a) reflective mode and, b) transmissive

1.17 Aim of This Work

With the discovery of conducting polymers both academia and industry have aimed to designand synthesize new CPs for organic electronics, photonics and biosensors. The goal of the researchers in the field of electrochromism is to synthesize polymers which switches between red, blue, green (RGB) colors, black and transmissive. Toppare research group successfully synthesized a polymer named as **PTBT** that possesses all RGB colors, black and transmissive. Despite its fascinating optical properties; multichromism, good optical contast, p and n dopability and high stability during kinetic studies, it exhibits relatively high switching time (2 s) [45].

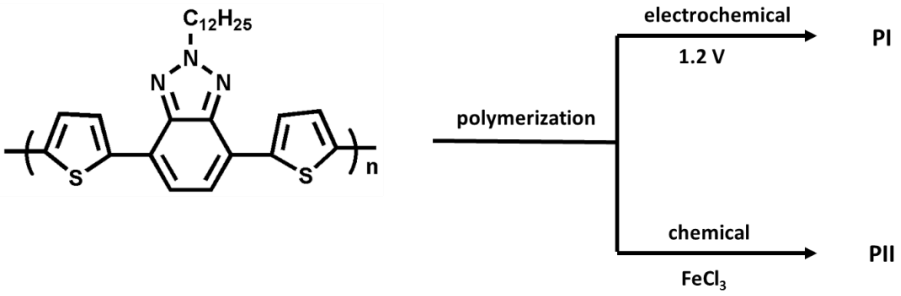

Figure 10. Synthesis of **PTBT**

In 2011, two novel benzotriazole (BTz) derivative polymers were synthesized by the same research group to enhance the optical properties and electrochromic properties of **PTBT** (**Figure 11).** The synthesizedbenzotriazole based polymers exhibited faster switching times than **PTBT**;for **PTBTTh** 1.5 s and for **PTBTPh** 1.6 s.[46].

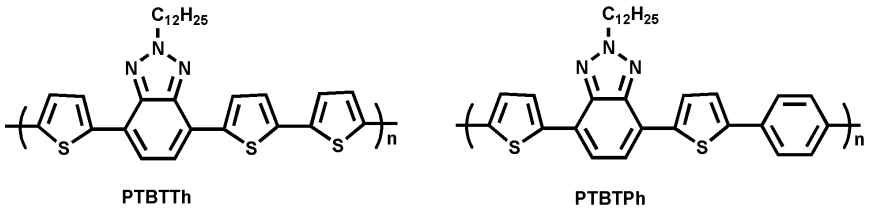

Figure 11. Chemical structuresof **PTBTTh** and **PTBTPh**

Up to now, thiophene unit has been commonly utilized as a π-bridge in BTz containing conjugated polymers architecture [47-58]. However, recent studies showed that selenophene substitution in the polymer backbone instead of thiophene is an effective approach to synthesize low band gap polymers with enhanced switching time and conductivity.Selenophene-bearing polymers showed enhanced planarity and extended conjugation length due to its less aromaticity. It was also found that the band gap of selenophene-based polymers was lower compared to other chalcogenophene derivatives because LUMO was predominantly lowered while the HOMO was not affected.These findings were supported by theoretical and experimental findings and attributed to small electronegativity difference between sulphur and selenium and lower ionization potential of selenium [59-66]. Therefore, it is noteworthy to state that usage of selenophene as π-bridge in BTz bearing conjugated polymers can be a useful strategy to synthesize low band gap polymers which also exhibit fast switching time. This study covers the syntheses of two novel polymers; poly(2-(2-octyldodecyl)-4-(selenophen-2-yl)-7-(5-(thiophen-2-yl)selenophen-2-yl)-2H-benzo[d][1,2,3]triazole) (**P-SBTTh**) and poly(2-(2-octyldodecyl)-4-(5-phenylselenophen-2-yl)-7-(selenophen-2-yl)-2H-benzo[d][1,2,3]triazole (**P-SBTTPh**) containing selenophene as a π-bridge in polymer backbone and also provides a synopsis of basic information about optical, electrochemical and electrochromic properties of polymers.

CHAPTER 2

2. EXPERIMENTAL

2.1 Materials and Methods

Selenophene, n-BuLi, tributyltinchloride, bis(triphenylphosphine)palladium(II) dichloride, n-bromosuccinimide (NBS, benzothiadiazole,), were purchased from Sigma-Aldrich Chemical Co. Ltd.. The commodity chemicals were used as received. Tetrahydrofuran (THF) and toluene were dried overNa/ benzophenone ketyl and freshly distilled prior to use.

2.2 Equipment

^{1}H and ^{13}C NMR spectra were recorded on a Bruker Spectrospin Avance DPX-400 Spectrometer with trimethylsilane (TMS) as the internal reference. The chemical shifts were reported in ppm relative to $CDCl_3$ at 7.26 and 77 ppm for the ^{1}H and ^{13}C NMR, respectively. The UV-vis spectra were recorded on Varian Cary 5000 UV–Vis spectrophotometer at room temperature. Cyclic voltammetry studies were carried out in a solution of 0.1 M of tetrabutylammonium hexafluorophosphate in anhydrous

acetonitrile (ACN) at a scan rate of 100 mV/s using a Voltalab 50 potentiostat in a three-electrode cell consisting of an ITO-coated glass slide as the working electrode, Pt wire as the counter electrode, and Ag wire as the pseudo reference electrode (calibrated against Fc/Fc+ (0.3 V)). Thermal properties of the polymers were analyzed by thermogravimetry analysis (TGA) (Perkin Elmer Pyris 1 TGA) under N2 atmosphere with a heating rate of 10 °C/min up to 300°C. Average molecular weight of the polymer was determined by gel permeation chromatography (GPC) using a Polymer Laboratories GPC 220.

2.3 Synthesis

Synthetic route forthe monomers and polymers were depicted in **Scheme 4.** The same procedure was applied for the synthesis of 4,7-dibromo-2-(2-octyldodecyl)-*2H*-benzo[1,2,3]triazole (**2**), which was described in detail in our previously published study [58]. BTz was anchored with long and branched solubilizing alkyl chain (2-octyldodecane) as the pendant group to ensure the solubility of the resulting polymers. Compound **2** wasthen coupled with tributyl(selenophen-2-yl)stannane (**1**) via Stille coupling to afford 2-(2-octyldodecyl)-4,7-di(selenophen-2-yl)-2H-benzo[d][1,2,3]triazole (**3**). Bromination of **3** was performed in the presence of NBS and DMF to synthesize 4,7-bis(5-bromoselenophen-2-yl)-2-(2-octyldodecyl)-*2H*-benzo[d][1,2,3]triazole (**4**). Then **4**was utilized for the syntheses of polymers. **P-SBTTh** was synthesized by Stille coupling copolymerization of **4** with 2,5-bis(tributylstannyl)thiophene in the presence of $Pd_2(PPh_3)_2Cl_2$ in THF solvent. **P-SBTPh** was synthesized by Suzuki coupling using **4** and 1,4-phenylenediboronic acid in the presence of $Pd(PPh_3)_4$ in toluene-water solvent system. The monomer and

copolymer molecular structures were confirmed by NMR spectroscopy. After successive purification via Soxhlett extraction with methanol, acetone and chloroform.

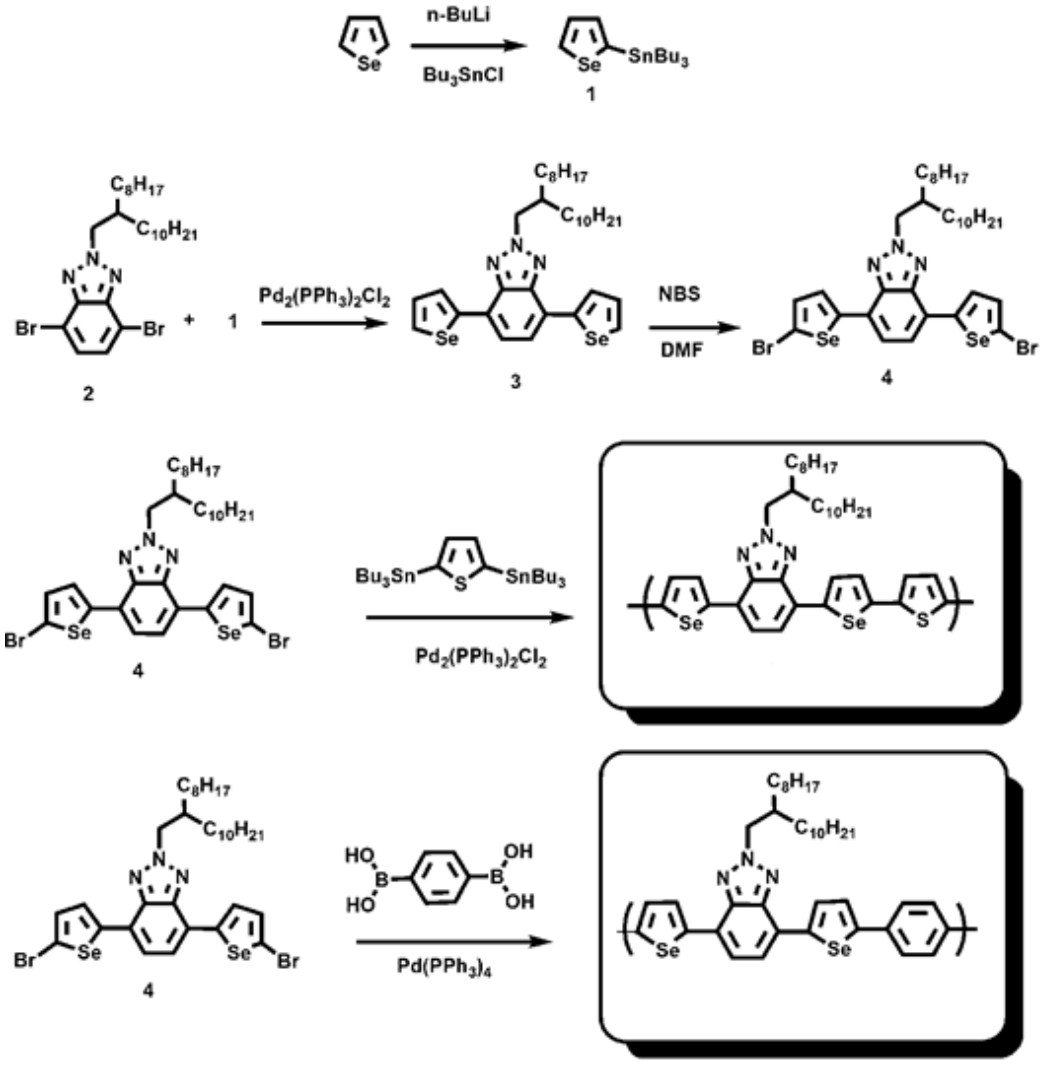

Scheme 4. Synthetic pathways of monomer and polymers

2.3.1 Synthesis of 9-(bromomethyl)nonadecane

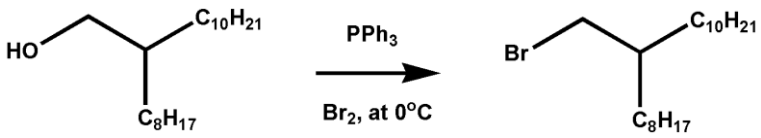

Figure 12. Synthesis of 9-(bromomethyl)nonadecane

2-Octyl-1-dodecanol (1.94 g, 6.50 mmol) was dissolved in CH_2Cl_2 (DCM) (50 mL) and triphenylphosphine (PPh_3) (1.79 g, 6.82 mmol) was added to solution at 0°C. Bromine (0.35 mL, 15.5 mmol) was added to reaction mixture and reaction stirred for half an hour at 0°C. Then, reaction was warmed to room temperature and reaction mixture was washed with $NaHSO_3$ and organic layer was further washed with distilled water and brine. The organic layer was dried over $MgSO_4$ and the solvent was evaporated under reduced pressure. Column chromatography on silica gel using hexane yielded colorless oil (2.23 g, 94%). ^{1}H NMR (400 MHz, $CDCl_3$), d (ppm): 3.37(d, *J*= 4.7 Hz, 2H), 1.52 (m, 1.46–1.57, 1H), 1.20 (m, 1.15–1.32, 32 H), 0.81(t, J =6.58 Hz, 6H).^{13}C NMR (400 MHz, $CDCl_3$), d (ppm): 39.6, 39.5, 32.59, 31.9, 29.8, 29.7, 29.6, 29.5, 29.4, 29.3, 26.6, 22.7, 14.1.

2.3.2 Synthesis of 4,7-dibromobenzo[c][1,2,5]thiadiazole

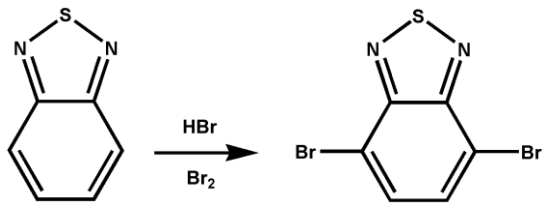

Figure 13. Synthesis of 4,7-dibromobenzo[c][1,2,5]thiadiazole

Benzo-1,2,5-thiadiazole (5.00 g, 36.7 mmol) was dissolved in HBr (47%)(30 mL). After, a solution of Br_2 (17.6 g, 110 mmol) in HBr (30 mL) was added slowly to reaction mixture at room temperature. After addition was completed, the reaction mixture was refluxed at 135 ^oC for overnight. Then the mixture was cooled to room temperature and filtered to obtain an orange solid residue. The residue was washed with $NaHSO_3$solution to consume excess Br_2. The crude was then dissolved in DCM and washed with brine. The organic layer was dried over $MgSO_4$ and the solvent was evaporated under reduced pressure. The obtained solid was washed with cold diethyl ether several times to afford 4,7-dibromobenzo[c][1,2,5]thiadiazole (9.7 g, yield 90%) as a yellow solid.

2.3.3 Synthesis of 3,6-dibromobenzene-1,2-diamine

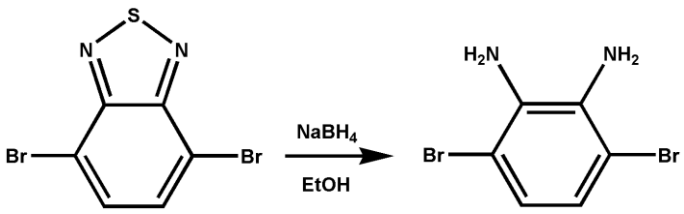

Figure 14. Synthesis of 3,6-dibromobenzene-1,2-diamine

.

4,7-Dibromobenzothiadiazole (5.0 g, 17 mmol) was dissolved in ethanol (EtOH) (50 mL) in 1000 mL round bottom flask. The mixture was cooled to 0^{o}C in an ice bath and $NaBH_4$ powder (25.7 g, 0.68 mol) was slowly added to reaction mixture.When gas evoluation was stopped, the reaction was warmed to room temperature and stirred for 20 hours. The solvent was evaporated and the residue was partitioned between diethyl ether and brine. The the organic phase was separated and the solvent was evaporated under reduced pressure to yield a faint yellow solid, 3,6-dibromobenzene-1,2-diamine(3.5 g, yield 80%).

2.3.4 Synthesis of 4,7-dibromo-2H-benzo[d][1,2,3]triazole

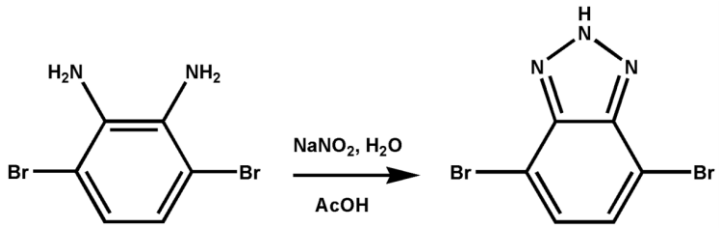

Figure 15. Synthesis of 4,7-dibromo-2-(2-octyldodecyl)-2H-benzo[d][1,2,3]triazole

To a solution of 3,6-dibromobenzene-1,2-diamine (5.00 g, 18.8 mmol) in 75 mL acetic acid (AcOH), a solution of $NaNO_2$(1.88 g, 20.7 mmol) in 36 mL H_2O was added slowly and the misxture was stirred for 20 minutes at room temperature. The precipitate was collected by filtration and washed with distilled water several times to afford 4,7-dibromo-2H-benzo[d][1,2,3]triazole as a pink powder (2.51 g, yield 48%).

2.3.5 Synthesis of 4,7-dibromo-2-(2-octyldodecyl)-2H-benzo[d][1,2,3]triazole

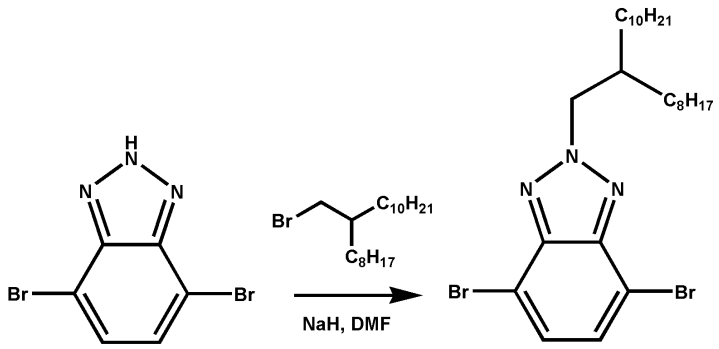

Figure 16. Synthesis of 4,7-dibromo-2-(2-octyldodecyl)-2H-benzo[d][1,2,3]triazole

4,7-Dibromo-2H-benzo[d][1,2,3]triazole (2.5 g, 9.0 mmol) was dissolved in dimethylformamide (DMF) (10 mL). Then, NaH (264 mg, 11.0 mmol) was added to reaction mixture at 0^{o}C and 9-(bromomethyl)nonadecane (3.45g, 9.56 mmol) was added at this temperature. The reaction was stirred at room temperature overnight. Water was added ant the reaction mixture was extracted with brine. The organic residue was dried over $MgSO_4$ and then, evaporation was done under reduced pressure. Column chromatography on silica gel with hexane and $CHCl_3$(1:2) yielded 4,7-dibromo-2-(2-octyldodecyl)-2H-benzo[d][1,2,3]triazole as a faint yellow oil (2.3 g, yield 40%).^{1}H NMR (400 MHz, $CDCl_3$), d (ppm): 7.36 (s,2H), 4.62 (d, J= 7.3 Hz, 2H), 2.26 (m, 1H), 1.15(m, 32H), 0.80 (m,6H). ^{13}C NMR (400 MHz, $CDCl_3$), d(ppm):140.3 , 128.2, 106.3, 56.6, 35.3, 29.3, 29.4, 29.3, 29.0, 27.5, 27.3, 27.2, 27.1, 27.0, 26.9, 23.5, 20.4, 20.3, 11.5.

2.3.6 Synthesis of Tributyl(selenophen-2-yl)stannane

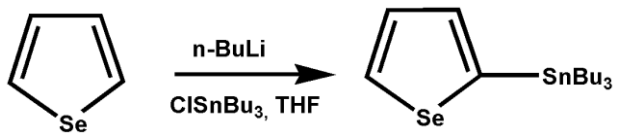

Figure 17. Synthesis of Tributyl(selenophen-2-yl)stannane

Selenophene (1.0, 7.6 mmol) was dissolved in dry tetrahydrofuran (THF) (20 mL)and the reaction mixture was cooled to -78^{o}C under argon atmosphere. 2.5 M n-BuLi in hexane (3.66 mL,39.6 mmol) was dropwisely added to reaction mixture. After addition of n-BuLi was completed, the reaction mixture was stirred for 1 hour at -78^{o}C. Then, stannyltributyltinchloride (2.21 mL, 8.15 mmol) was slowly added to the reaction mixture at -78^{o}C. After addition was completed, the reaction mixture was stirred for 1.5 hours at -78^{o}C, warmed to room tempeatureand stirred overnight. The reaction mixture was poured tosaturated solution of $NaHCO_3$ and organic phase was separated, washed with brine and dried over $MgSO_4$. The residue was purified by neutral alumnia column chromatography with hexane as the eluent to obtain colorless oil of tributyl(selenophen-2-yl)stannane (2.56 g, yield 80%).%). ^{1}H NMR (400 MHz, $CDCl_3$), d (ppm): 8.5 (d, J=4.8,1H), 7.7 (m, J= 7.3 Hz, 2H), 1.8 (m,6H), 1.55(m, 6H), 1.1 (m,6H), 0.9 (t, 9H)

2.3.7 Synthesisof 2-(2-octyldodecyl)-4,7-di(selenophen-2-yl)-2H-benzo[d][1,2,3]triazole

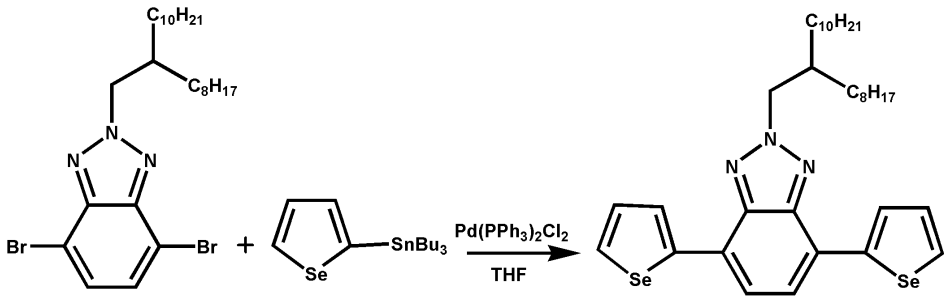

Figure 18. Synthesis of 2-(2-octyldodecyl)-4,7-di(selenophen-2-yl)-2H-benzo[d][1,2,3]triazole

4,7-Dibromo-2-(2-octyldodecyl)-2H-benzo[d][1,2,3]triazole (852 mg, 1.53 mmol) and tributyl(selenophen-2-yl)stannane (2.8 g, 6.7 mmol) were dissolved in THF (100 mL). Bis(triphenylphosphine)palladium(II)dichloride (135 mg, 0.19 mmol) was added into the solution and the reaction mixture was refluxed for 18 h under argon atmosphere. After the reaction was completed, solvent was removed under reduced pressure. Column chromatography was performed by silica gel with petroleum ether and DCM (10:1) and product was obtained as a yellow solid (790 mg, yield % 78). ^{1}H NMR (400 MHz, $CDCl_3$) , δ (ppm): 8.1 (dd , J_1=0.95 Hz, J_2=2.90 Hz, 2H) , 7.9 (dd , J_1=0.95 Hz, J_2=4.68, 2H) 7.5 (s , 2H), 7.32 (dd, J_1=1.73 Hz, J_2=3.89 Hz, 2H) 4.64 (d, J=6.42 Hz, 2H), 2.18 (m, 2.14–2.23, 1H), 1.25 (m, 1.12–1.32, 32H), 0.78 (m, 0.74–0.82, 6H). ^{13}C NMR (400 MHz, $CDCl_3$), δ (ppm): 143.7, 140.3, 130.0, 128.9, 126.6, 123.9, 121.3, 75.6, 75.3, 37.7, 30.5, 30.4, 30.1, 28.4, 28.2, 28.1, 27.9, 24.9, 21.3, 12.7.

2.3.8 Synthesis of 4,7-bis(5-bromoselenophen-2-yl)-2-(2-octyldodecyl)-2H-benzo[d][1,2,3]triazole

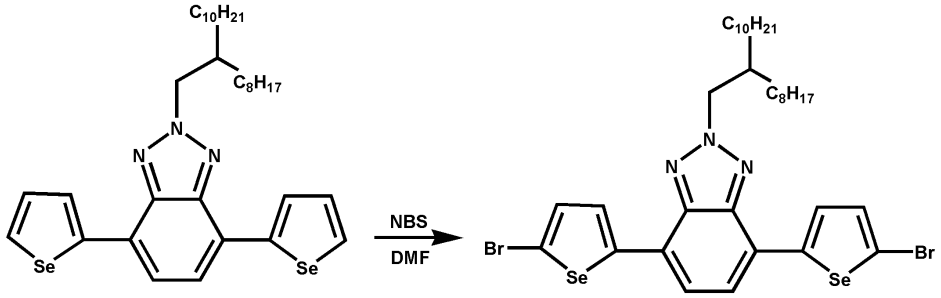

Figure 19. Synthesis of 4,7-bis(5-bromoselenophen-2-yl)-2-(2-octyldodecyl)-2H-benzo[d][1,2,3]triazole

2-(2-Octyldodecyl)-4,7-di(selenophen-2-yl)-2H-benzo[d][1,2,3]triazole (790 mg, 1.20 mmol) was dissolved in anhydrous DMF (30 ml). N-bromosuccinimide (517 mg, 3.10 mmol) was added and the mixture was stirred at room temperature under argon atmosphere for 18 hours. The solvent was removed by under reduced pressure, the R-residue was dissolved in $CHCl_3$ and washed with water. The organic layer was separated, dried with $MgSO_4$ and the solvent was evaporated. Column chromatography was performed by silica gel with $CHCl_3$ and the product was obtained as a dark yellow solid (957 mg, yield % 97). ^{1}H NMR (400 MHz, $CDCl_3$), δ (ppm): 7.7 (d, *J*=4.22 Hz, 2H) 7.46 (s, 2H) 7.25 (d, *J*=4.22 Hz, 2H) 4.65 (d, *J*=6.42 Hz, 2H), 2.18 (m, 2.14–2.22, 1H), 1.25 (m, 1.12–1.35, 32H), 0.79 (m, 0.73–0.85, 6H). ^{13}C NMR (400 MHz, $CDCl_3$), δ (ppm): 132.6, 126.3, 133.5, 132.6, 130.7, 129.0, 126.1, 114.8, 77.3, 77.0, 76.7, 31.9, 31.5, 29.9, 29.6, 29.3, 26.3, 22.7, 14.1.

2.3.9 Synthesis of P-SBTTh

4,7-Bis(5-bromoselenophen-2-yl)-2-(2-octyldodecyl)-2H-benzo[d][1,2,3]triazole (340 mg, 0.42 mmol) and 2,5-bis(tributylstannyl)thiophene (280 mg, 0.42 mmol) were dissolved in anhydrous THF under argon atmosphere and heated to reflux. Bis(triphenylphosphine)palladium(II)dichloride (0.125 g) was added to reaction mixture and the reaction was refluxed for three days. Polymer was precipitated with methanol and Soxhlett extraction was carried out with acetone and hexane. Polymer was recovered by chloroform and dried under vacuum.**P-SBTTh** was obtained as a purple solid with a yield of 35.4 % (110 mg). GPC: number average molecular weight (Mn): 2500, molecular average molecular weight (Mw): 3000, polydispersity index (PDI): 1.2. ^{1}H NMR (400 MHz, $CDCl_3$), δ (ppm): 8.02 (BTz), 7.64 (Thiophene), 7.47 (Selenophene), 7.37 (Selenophene) 4.7 (N–CH_2, BTz), 2.24 (–CH), 1.4-0.9 (-CH_2), 0.76 (-CH_3)

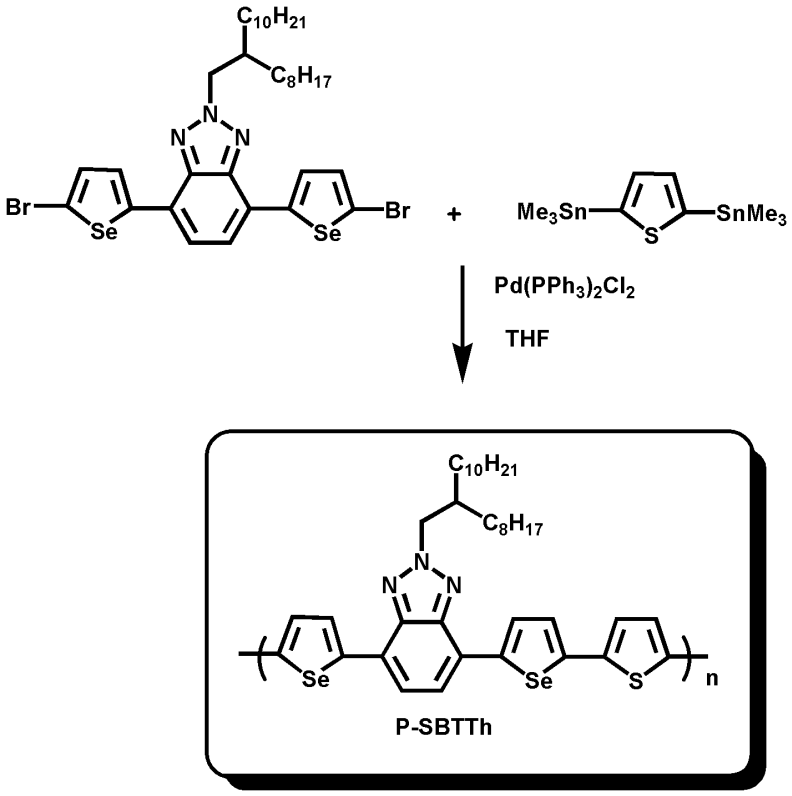

Figure 20. Synthesis of **P-SBTTh**

2.3.10 Synthesis of P-SBTPh

4,7-Bis(5-bromoselenophen-2-yl)-2-(2-octyldodecyl)-2H-benzo[d][1,2,3]triazole (670 mg, 0.82 mmol) and 1,4-phenylenediboronic acid (136 mg, 0.82 mmol) potassium carbonate (K_2CO_3, 2 M in H_2O), toluene (3: 2 toluene : water) (50 mL), $Pd(PPh_3)_4$ (5 mol %), and tetrabutylammonium iodide ($N(Bu)_4I$, (1 mol %) were refluxed under argon atmosphere for 24 hours. The solvent was removed and the residue was poured into water and extracted with $CHCl_3$. The solvent was evaporated under reduced pressure. Polymer was precipitated in methanol and Soxhlett extraction was carried out

with acetone and hexane. Polymer was recovered by chloroform and dried under vacuum. **P-SBTPh** was obtained as a purple solid with a yield of 16.6 % (100 mg). GPC: Number Mn: 15400, Mw: 19200, PDI: 1.25. ^{1}H NMR (400 MHz, $CDCl_3$), δ (ppm): 8.03 (BTz), 7.64 (Selenophene), 7.57 (Selenophene), 7.3 (Benzene), 4.72 (N-CH_2), 2.26 (-CH), 1.3-1.0 (–CH_2), 0.9-0.7 (-CH_3).

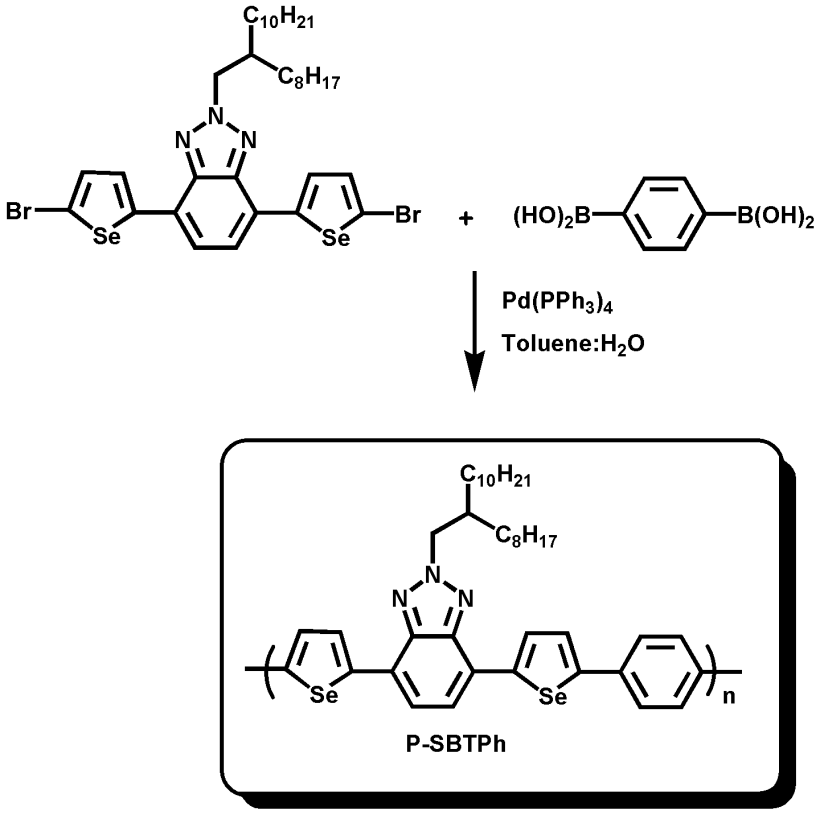

Figure 21. Synthesis of **P-SBTPh**

2.4 Characterization ofConducting Copolymers

2.4.1 Gel Permeation Chromatography

Gel permeation chromatography **(GPC)** is a chromotographic technique that aims todetermine the molecular weight of the polymers and it involves solid stationary phase and liquid mobile phase. GPC differs from other chromotographic techniques with its separation mechanism. The separation mechnanism of GPC relies on the size of the polymer molecules in solution rather than the chemical interactions between stationary phase and particles.

2.4.2 Thermal Analysis

Thermal properties of the polymers were examined by thermal gravimetry analysis (TGA) and differential scanning calorimetry (DSC) under nitrogen atmosphere. DSC studies were perfomed with Perkin Elmer Differential Scanning Calorimetry. In DSC analysis, heat capacity of polymer by temperature change was examined. DSC analysis allows detection of glass transition temperature (T_g), melting temperature (T_m).

The mass of polymer decreases upon heating and TGA studies monitor the mass change as a function of temperature. TGA studies give information about decomposition temperature of polymer (T_d) and quantity of weight loss. Thermal gravimetric analysis was performed with Perkin Elmer Pyris 1 Thermal Gravimetry Analysis.

2.4.3 Cyclic Voltammetry

Cyclic voltammetry (CV) is a multi-purpose electroanalytical technique that examines the electroactivity of compounds and also CV is used for the electropolymerization of monomers. CV gives information about p or n type doping potentials and their corresponding dedoping potentials of electroactive materials.

CV comprises of cycling the potential applied onelectrode immersed in solution and measuring the resulting current. The potential of working electrode is controlled with respect toa reference electrode. The controlled potential utilized across the reference and working electrodesis the initiation for the polymerization. The excitation signal is a linear potential with a triangular waveform as shown in **Figure22.** The potential sweeps between any two values; as switching potentials. The current response is monitored as a function of applied potential,**Figure22** represents a simple cyclic voltammogram.

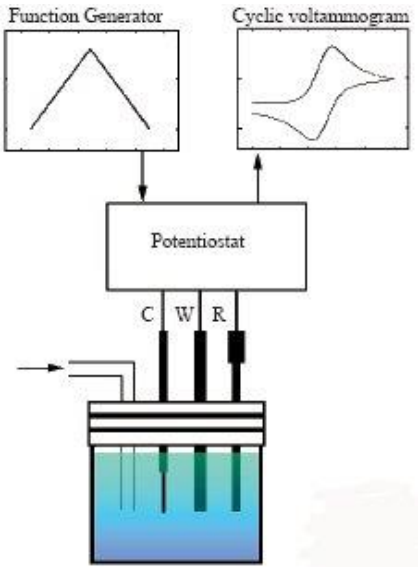

Figure 22. Representative cyclic voltammetry (CV)

2.4.4 Spectroelectrochemistry

Spectroelectrochemical analysis combines the spectoscopic and electrochemical analyses. In order to demonstrate the color and the color changes that occur upon doping porcesses, spectroelectrochemisrty analysis is utilized. In addition, spectroelectrochemistry analysis gives information on maximum absorption wavelength (λ_{max}), optical band gap (E_g^{opt}) and intergap states named as bipolarons and polarons.

To perform spectroelectrochemical analysis, a polymer coated ITO (indium tin oxide) is placed in a cuvvette which involves a reference electrode (Ag/Ag^+)and Pt wire as the counter electrode. The set up cell is then combined with a potentiostat and the polymer is oxidized upon applied potential, simultaneously the absoption spectrum of the polymer is recorded.

2.4.5 Kinetic studies

Switching time and optical contrastare important parameters for an efficient electrochemical device of conducting polymers. To investigate the switching time and optical contrast of the polymer, a square wave potential step coupled with spectroscopy method konown as chronoamperometry was applied. The transmittance change between oxidized and reduced states is named as *''optical contrast''*. The time is needed for a polymer to oxidize from its reduced state is known as *''switching time''*.

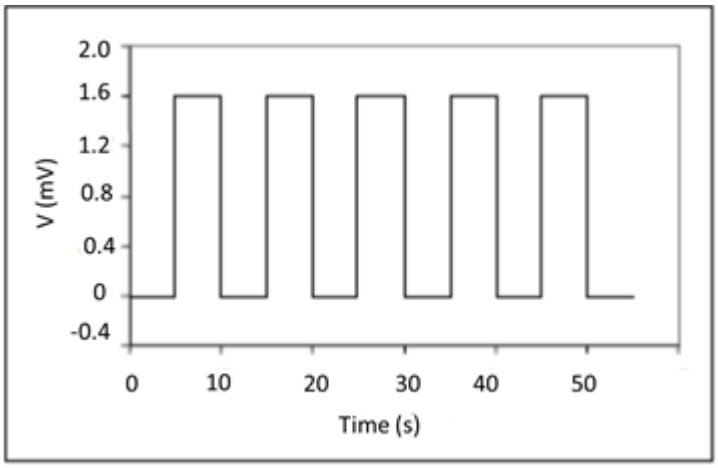

Figure 23. Representative square wave voltammetry

CHAPTER 3

3. RESULTS AND DISCUSSION

3.1 Electrochemical Characterization of Copolymers

3.1.1 Electrochemical Properties of P-SBTTh

Cyclic voltametry is a versatile instrument utilized to determine redox behavior and HOMO and LUMO energy levels of the conjugated polymers. Therefore, electronic behavior of **P-SBTTh**was determined by cyclic voltammetry (CV). **P-SBTTh** was dissolved in chloroform (5 mg\mL) and spray coated on ITO electrode. Then CV was performed in three-electrode cell consisting of an ITO-coated glass slide as the working electrode and a Pt wire as the counter electrode. CV measurements were carried out in 0.1 M $TBAPF_6$ /ACN solution at a scan rate of 100 mV/s (**Fig. 24**). Electrochemical properties of polymer weresummarized in **Table 1.**

P-SBTTh showed only p-doping property. **P-SBTTh** showed one oxidation potential at 0.93 V and a reversible reduction couple at 0.62 and 0.94 V. HOMO energy level of **P-SBTTh** was determined from onset potential of oxidation, which was observed at 0.69 V. HOMO energy levelof **P-SBTTh**was calculated from HOMO=$(4.75+E_{onset}^{ox})$ and found as -5.44 eV, respectively. Relative LUMO energy level of polymer was

calculated by using optical band gap and HOMO energy level due to absence of n-doping and determined as -3.9 eV.

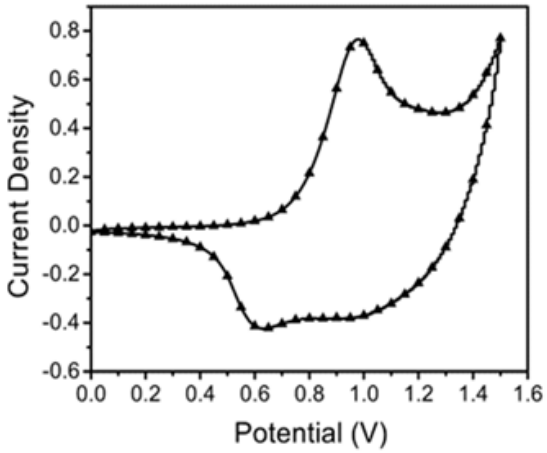

Figure 24. Cyclic voltammograms of **P-SBTTh** in 0.1 M $TBAPF_6$/ACN solvent-electrolyte couple witha scan rate of 100 mV/s

Table 1. Summary of optical and electrochemical properties of **P-SBTTh**

Electrochemical Properties			Optical Properties		
Polymer	HOMO (eV)	LUMO* (eV)	Thin film λ_{max} (nm)	Solution λ_{max} (nm)	E_g^{opt} (eV)
P-SBTTh	-5.44	-3.90	550	544	1.54

*LUMO energy level is calculated from optical data.

3.1.2 Electrochemical Properties of P-SBTPh

Electronic behavior of **P-SBTPh**was determined by cyclic voltammetry (CV). Polymers were dissolved in chloroform (5 mg\mL) and spray coated on ITO electrode. Then CV was performed in three-electrode cell consisting of an ITO-coated glass slide as the working electrode, Pt wire as the counter electrode. CV measurements were carried out in 0.1 M $TBAPF_6$ /ACN solution at a scan rate of 100 mV/s (**Fig. 25**). Electrochemical properties of polymer was summarized in **Table 2.**

P-SBTPh also showed only p-doping property. Although, **P-SBTTh** has thiophene ring in its backbone that is more electron rich compared to benzene, **P-SBTPh** oxidation potential was also observed at 0.93 V. HOMO energy level of**P-SBTPh** was determined from onset potential of oxidation, which was observed at 0.79 eV. HOMO energy level of**P-SBTPh** was calculated from HOMO=(4.75+ E_{onset}^{ox}) and found as -5.54 eV, respectively. Relative LUMO energy level of polymerwas calculated using optical band gap and HOMO energy level due to absence of n-doping and determined -3.92 eV.

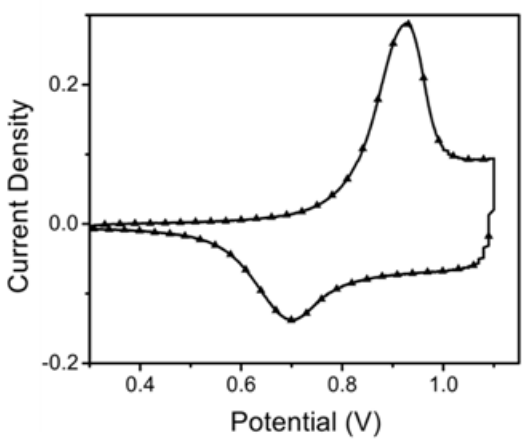

Figure 25. Cyclic voltammograms of **P-SBTPh** in 0.1 M $TBAPF_6$/ACN solvent-electrolyte couple with a scan rate of 100 mV/s.

Table 2. Summary of optical and electrochemical properties of **P-SBTPh**

Electrochemical Properties			Optical Properties		
Polymer	HOMO (eV)	LUMO* (eV)	Thin film λ_{max} (nm)	Solution λ_{max} (nm)	E_g^{opt} (eV)
P-SBTPh	-5.54	-3.92	537	516	1.62

*LUMO energy level is calculated from optical data.

When we compared oxidation potential of **P-SBTTh**and **P-SBTPh** with their thiophene counterparts, namely **P-TBTTh** and **P-TBTPh,** their oxidation potentials were observed at lower potentials. Oxidation potentials of **P-TBTTh** and **P-TBTPh**were 1.04 and 1.12 eV respectively[55]. Difference in oxidation potentials can be attributed to electron rich nature of selenophene compared to thiophene. Although **P-TBTTh** and **P-TBTPh** bear dodecyl group as the side chain, this does not hinder the comparison since substitution of branched alkyl chain has no effect on optical and electrochemical properties whereas it mostly affects physical properties [68,69]. Therefore, most of the changes in electrochemical properties are the result of different chalcogenophene rings in polymer structure.

3.1.3 Scan Rate Studies of Polymers

The scan rate dependence of the anodic and cathodic peak currents was studied in a electrolyte solution at different scan rates (**Figure 26**and **Figure 27**). In this system, diffusion from solution to the surface area of the polymer does not take place and it is

constant. The change in the peak current of the polymer is discussed by the following equation:

$$i_p = n^2 F^2 \Gamma \nu / 4RT$$

The linear relation between peak current intensities of polymer and scan rate is obsereved for non-diffusion controlled mechanism. The peak current is linearly dependent on the scan rate. A linear relationship was found between the peak current and the scan rate for **P-SBTTh** and **P-SBTPh**. This relationship indicates that the electroactive polymer films were well adhered and the redox processes were non-diffusion controlled.

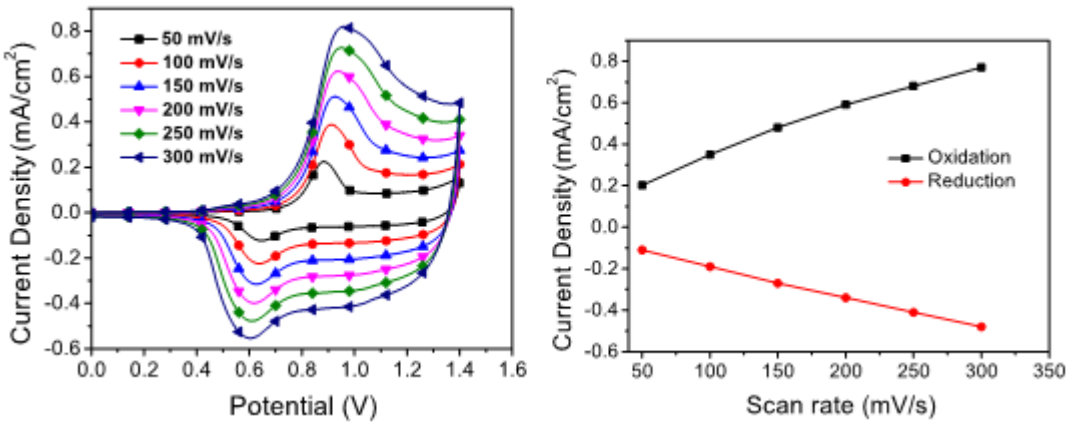

Figure 26. Cyclic voltammograms of **P-SBTTh** in 0.1 M $TBAPF_6$/ACN at scan rates of 100, 150, 200, 250 and 300 mV/s.

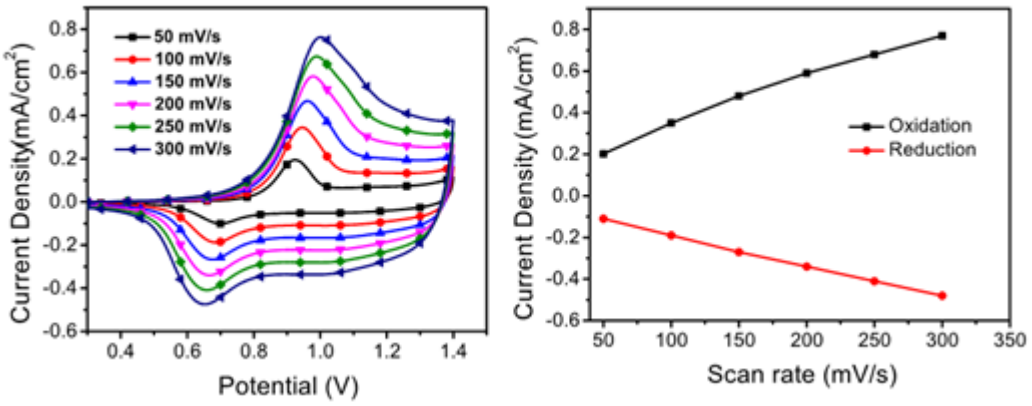

Figure 27. Cyclic voltammograms of **P-SBTPh** in 0.1 M $TBAPF_6$/ACN at scan rates of 100, 150, 200, 250 and 300 mV

3.1.4 Optical Properties of P-SBTTh and P-SBTPh

Optical properties of polymers were investigated in thin form and in dilute chloroform solution and presented in **Figure 28.**All relevant data were summarized in **Table 3.** The maximum absorptions for **P-SBTTh** and **P-SBTPh** in solution were observed at 544 nm and 516 nm respectively. The absorption spectra of the polymer film of **P-SBTPh** (21nm) showed obvious red shift relative to the one recorded in solution. This phenomenon is the result of the molecular organization in the thin film to form more ordered structures and well-ordered intermolecular interaction in solid state. It is noteworthy to state that **P-SBTTh** did not show any meaningful red shift in thin film form, instead a slightly broadened absorption peak was observed. This can be ascribed to small reorganization in thin film and pre-aggregation in solution [70].

When optical properties of **P-SBTTh** and **P-SBTPh** were compared with their thiophene anologs, 23 nm and 21 nm red shifts were observed in maximum absorptions of **PTBTTh** and **PTBTPh** respectively. Incorporation of selenophene in polymer

backbone not only causes a red shift but also lowers the optical band gap compared to thiophene analogs. Differences as much as 0.21 eV and 0.23 eV in the optical band gaps of **PTBTTh** and **PTBTPh** were observed. These findings can be attributed to the shorter inter-ring C–C bonds of selenophene containing polymers compared to thiophene analogs. Therefore, the quinoid structure will make a significantly greater contribution to the ground state of **P-SBTTh** and **P-SBTPh** compared to **PTBTTh** and **PTBTPh** and energetically less stable quinoidal form can result in the reduction of band gap [59,60].

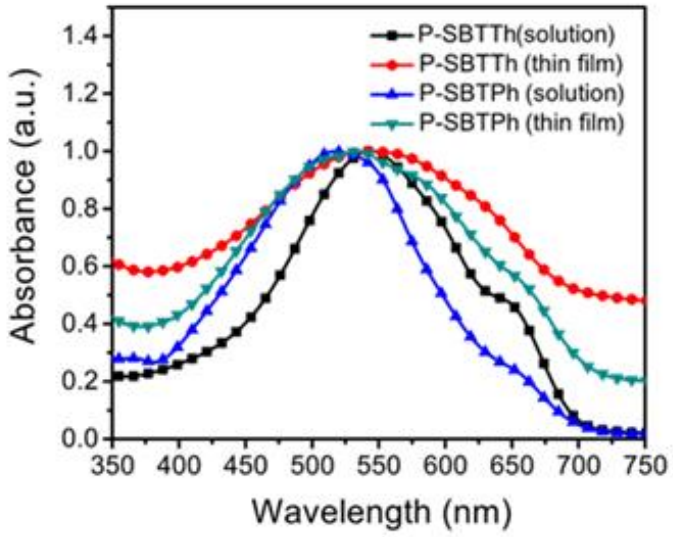

Figure 28. Normalized absorption spectra **of P-SBTTh** and **P-SBTPh** in chloroform solution and in thin film form

Table 3. Summary of optical properties of polymers

.

Optical Properties		
Polymer	Thin film λ_{max} (nm)	Solution λ_{max} (nm)
P-SBTTh	550	544
P-SBTPh	537	516

3.1.5 Spectroelectrochemical Properties of P-SBTTh

Spectroelectrochemistry studies were performed to gain a deeper idea on the changes in the optical properties during doping process. Therefore, polymer was spray coated and absorbance changes were studied by increasing the potential gradually from 0.0 V to 1.3 V for **P-SBTTh**in 0.1 M $TBAPF_6$/ACN electrolyte-solvent couple by UV-Vis-NIR spectroscopy. As shown in **Figure 29**, **P-SBTTh**exhibited one absorption band arising from π–π* transition. **P-SBTTh** has a dominant red shifted absorption centered at 550 nm with an onset of 806 nm. The optical band gap (E_g^{opt}) was calculated from onset of absorption of the thin film and estimated as 1.54 eV for **P-SBTTh**. **P-SBTTh**was oxidized in a stepwise manner, neutral state absorption started to decrease and new bands intensified in the NIR region at around 800 nm and 1280 nm due to formation of polarons and bipolarons. **P-SBTTh**exhibited purple color in its neutral states and stepwise oxidation caused the observation of different colors. Transmissive grey color was observed for **P-SBTTh** in their oxidized states. The absence of transparent color in bleached state can be attributed to the tailoring of polaron peaks in visible region.

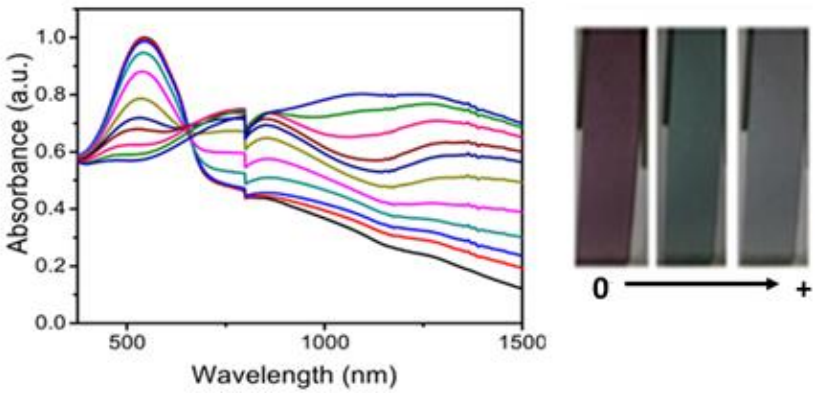

Figure 29. UV–Vis–NIR spectra and colors of **P-SBTTh** potentials between 0 and 1.3 V.

3.1.6 Spectroelectrochemical Properties of P-SBTPh

For the same purpose, spectroelectrochemistry studies were performed for the **P-SBTPh.** It was spray coated and absorbance changes were studied by increasing the potential gradually from 0.0 V to 1.35 V in 0.1 M $TBAPF_6$/ACN electrolyte-solvent couple by UV-Vis-NIR spectroscopy. As shown in **Figure 30**, **P-SBTPh**exhibited one absorption band arising from π–π* transition. **P-SBTPh** revealed a maximum absorption band at 516 nm with an onset of 764 nm. The optical band gapof **P-SBTPh**was calculated from onset of absorption of the thin film and estimated as 1.62 eV. Even though, **P-SBTPh** had an extended π-conjugation length compared to **P-SBTTh**, it had larger band gap. This indicates that the bandgaps were predominantly determined by the electron-donating ability of the additional donor units (benzene < thiophene) in the polymer backbones. Then, **P-SBTPh** was stepwise oxidized, neutral state absorptions started to decrease and new bands were intensified in the NIR region at around 800 nm and 1280 nm for **P-SBTTh** and 770 nm and 1200 nm for **P-SBTPh** due to formation of polarons and bipolarons. Both polymers exhibited purple color in their neutral states and stepwise oxidation caused the observation of different colors.

Transmissive grey color was observed for both polymers in their oxidized states. The absence of transparent color in bleached state can be attributed to the tails of polaron peaks in the visible region.

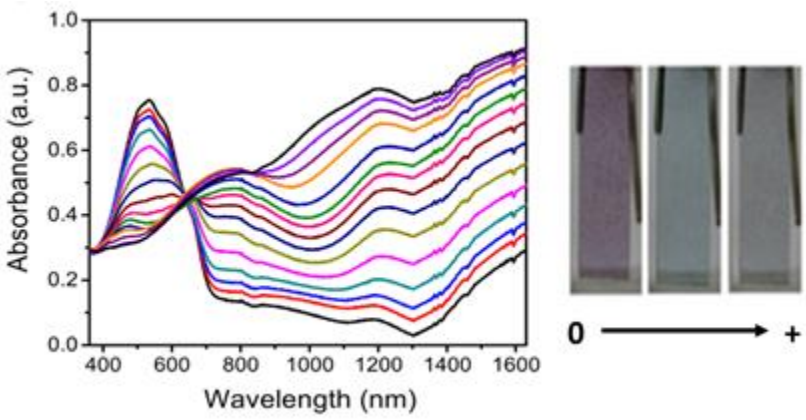

Figure 30. UV–Vis–NIR spectra and colors of **P-SBTPh** potentials between 0 and 1.35 V.

3.1.7 Kinetic Properties of P-SBTTh and P-SBTPh

In addition to optical, electrochemical and spectroelectrochemical properties, switching times and optical contrast are other important aspects for electrochromic device applications. Therefore, chronoamperometry studies of polymers were performed to calculate optical transmittance and switching times by stepping potentials between neutral and oxidized states with residence times of 1 s for **P-SBTTh** and 5 s for **P-SBTPh**. Optical contrast and switching times of the **P-SBTTh** in different wavelengths were summarized in **Table 4** and shown in **Figure 31**.**P-SBTTh** revealed 36 % and 37 % optical contrasts at 550 and 1280 nm. For **P-SBTPh,** optical properties and switching times were summarized in **Table 5** andshown in **Figure 32P-SBTPh**revealed lower optical contrast values in visible and NIR regions compared to **P-SBTTh** and

revealed 17 % in visible region (530 nm) and 14 % and 33 % in NIR region (770 and 1200 nm). Switching times were determined and calculated in different wavelengths for **P-SBTTh** and **P-SBTPh** and summarized in **Table 2.**Switching times of both polymers were less than 1 second. Calculated switching times of **P-SBTTh** were 0.6 s (550 nm) and 0.7 s (1280 nm). **P-SBTPh** showed fast switching times compared to **P-SBTTh** and switched between neutral and oxidized regimes in 0.2 s (530 nm), 0.4 s (770 nm), and 0.4 s (1200 nm).

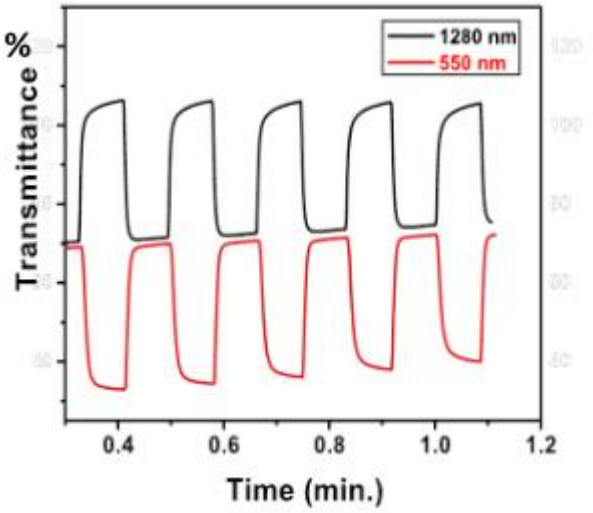

Figure 31. Percent transmittance change and switching times of **P-SBTTh** in 0.1 M $TBAFP_6$/ACN solution at its maximum wavelengths

Table 4. Optical contrast and switching times of the **P-SBTTh**

Polymer	Optical Contrast (ΔT%)	Switching time (s)
P-SBTTh	37 (1280 nm) 36 (550 nm)	0.7 0.6

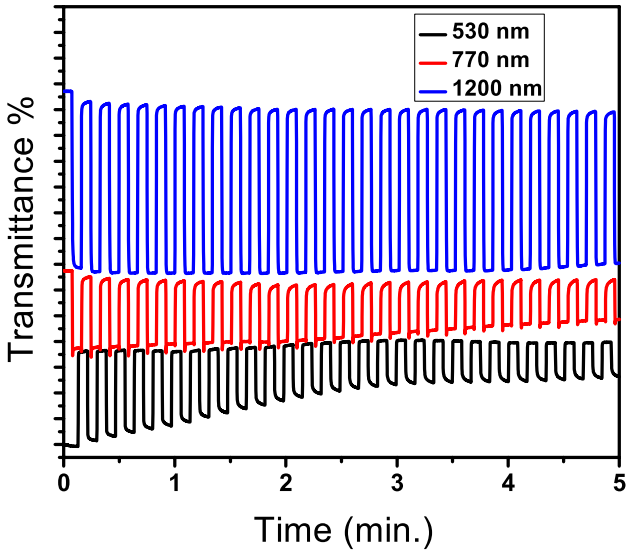

Figure 32. Percent transmittance change and switching times of **P-SBTPh** in 0.1 M $TBAFP_6$/ACN solution at its maximum wavelengths

Table 5. Optical contrast and switching times of the **P-SBTPh**

Polymer	Optical Contrast (ΔT%)	Switching time (s)
P-SBTPh	33 (1200 nm)	0.4
	14 (770 nm)	0.4
	17 (530 nm)	0.2

Both polymers exhibited moderate stability during kinetic studies. The reason for this can be explained by redox processes where polymers films are oxidized and reduced by insertion and extraction of ions in polymer film [69]. Therefore any remaining ions on polymer film can result in an irreversible redox process creating a stability problem. Although, incorporation of long alkyl chain can result in an increase in effective conjugation length and processability of polymer, conversely it may also hinder the exertion of counter ions from polymer backbone.

Although polymers showed moderate stability,they exhibited fascinating switching times. **P-SBTPh** showed outstanding switching times (0.2 s at 530 nm). To the best of our knowledge switching time of **P-SBTPh** is the fastest data measured up to now in all benzotriazol containing polymers. In addition to fast switching times, this polymer showed high stability at NIR region with reasonable optical contrast. By keeping in mind that the most electrochromic device (ECD) application needs fast switching times such as video displays (30-50 ms), information displays, e-readers, and point-of-purchase advertising (100-500 ms), so that **P-SBTPh** can be a reasonable candidate for NIR device applications in terms of fast switching time (0.4 s) with reasonable optical contrast.

3.1.8 Thermal Analysis

Thermal behaviors of polymers were examined by thermogravimetry analyses (TGA) under nitrogen atmosphere with a heating rate of $10^{o}C\ min^{-1}$. 5% mass loss was observed at 422°C for **P-SBTTh** and 5 % weight loss was observed at 370°C for **P-SBTPh**. Differential scanning calorimetry (DSC) was utilized to characterize the

thermal transitions in the polymers and **P-SBTTh**did not show any phase transition. **P-SBTPh** revealed a glass transition-like feature at 143 °C.

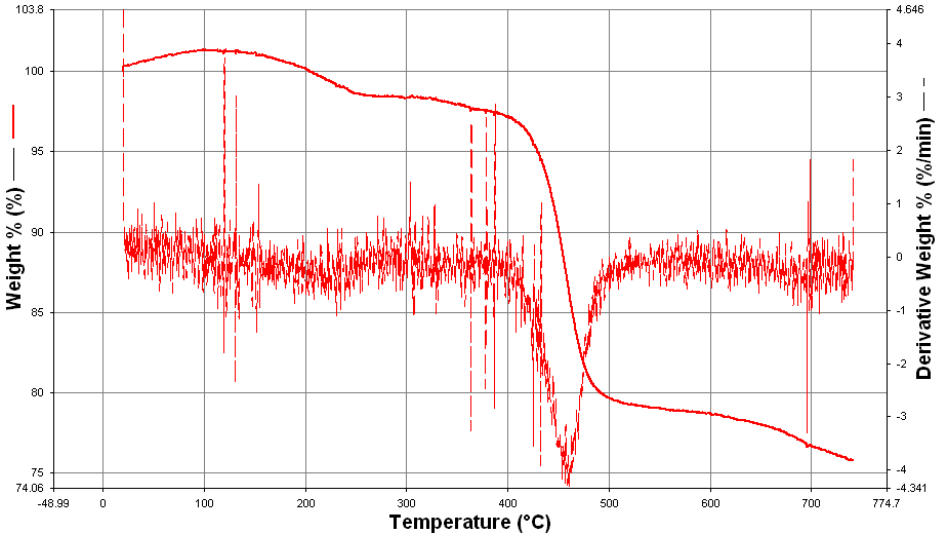

Figure 33. TGA result of **P-SBTTh**

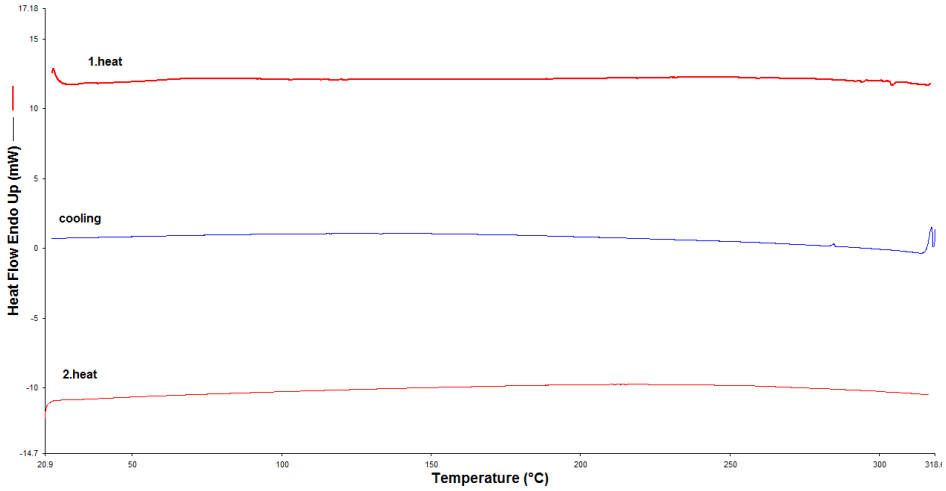

Figure 34. DSC result of **P-SBTTh**

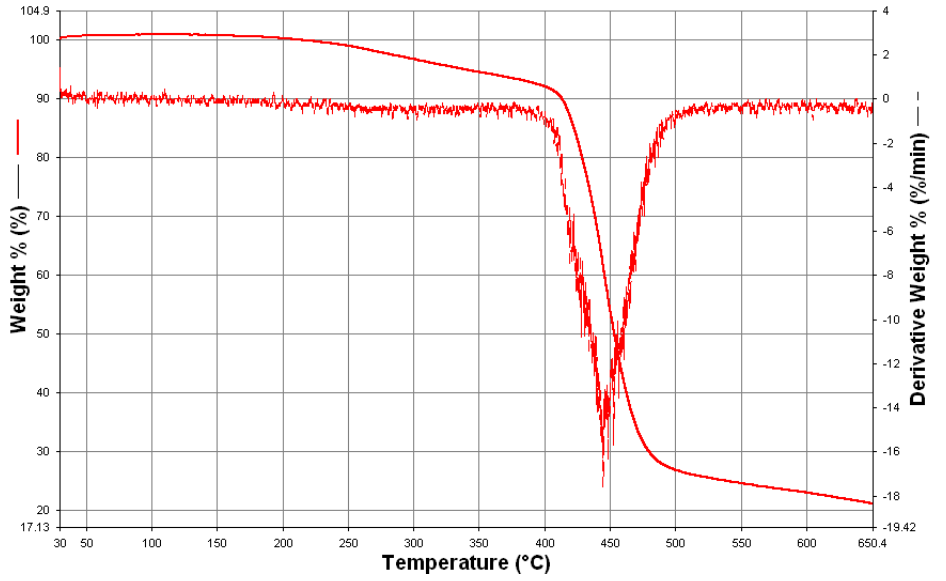

Figure 35. TGA result for **P-SBTPh**

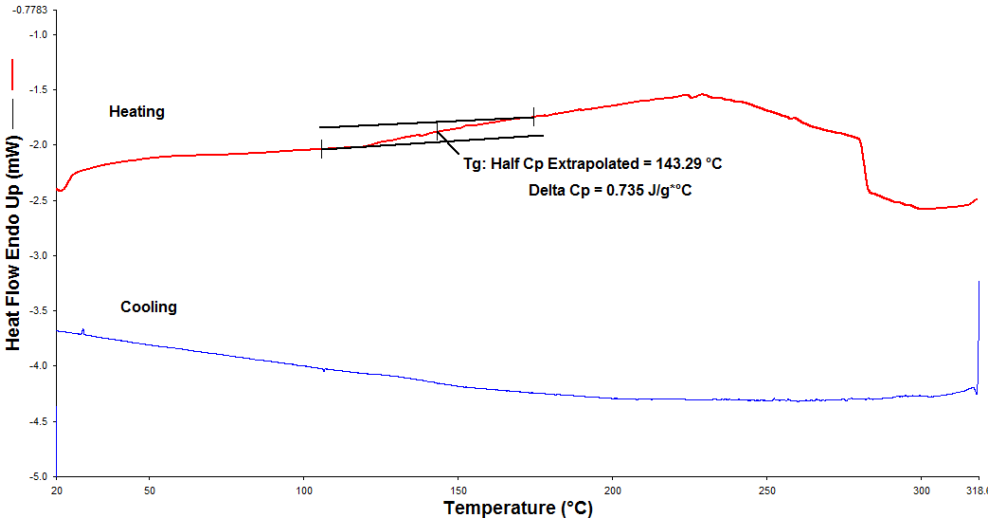

Figure 36. DSC result of **P-SBTPh**

CHAPTER 4

CONCLUSION

Two novel polymers containing selenophene as a π-bridge were synthesized via Stille and Suzuki coupling reactions. Selenophene incorporation in polymer backbone resulted in several changes in optical and electronic properties of BTz based polymer. It caused low band gap and red shifted absorption spectra compared to their thiophene analogs.Both polymers exhibited multichromism switching between purple, blue and highly transmissive grey color. Kinetic studies indicated that both polymers showed moderate stability butthey exhibited a fascinating property in terms of switching times.Especially, switching time of**P-SBTPh** atUV-vis region is the fastest data reported up to now in all benzotriazol based copolymers. In addition to fast switching times, this polymer showed high stability at NIR region with reasonable optical contrast (33%). Therefore,structural modification, done by insertion of different chalcogenophene rings in the polymer backbone, seems a reasonableway tocontrol optical, electrochemical and electrochromic properties of BTz based polymers. Therefore, further investigation of selenophene containing materials is needed to. From this perspective, design and synthesis of new materials are crucial for their use in different applications.

REFERENCES

1. T. P. Nguyen, P. Destruel. Electroluminescent Devices Based on Organic Materials and Conjugated Polymers. In Handbook of Luminescence, Display Materials, and Devices. *Organicc, American Scientific Publishers, Stevenson Ranch, CA*Vol.1, Pg.5, 2003.
2. P. B. Armstrong. The Design of Organic Polymers and Small Molecules to Improve the Efficiency of Excitonic Solar Cells.*University of California, Berkeley, Chemistry Department.* Pg.2, 2010.
3. J. Rocali. Advances in the Molecular Design of Functional Conjugated Polymers, In the Hanbook of Conducting Polymers, 2nd Ed.;A. T. Skotheim, R. L. Elsenbaumer, J. R. Reynolds. Eds.; Marcel Dekker, *Inc: New York.*311-341, 1998.
4. H. A. M. van Mullekom,J. A. J. M. Vekemans, E. E. Havinga,E. W. Meijer. Developments in the Chemistry and Band Gap Engineering of Donor-Acceptor Substituted Conjugated Polymers.*Mater. Sci. Eng.* (32)1-40, 2001.
5. S. C. Rasmussen,K. Ogawa,S. D. Rothstein, Synthetic Approaches to Band Gap Control in Conjugated Polymeric Materials.,*In the Handbook of organic Electronics and Photonics*; Nawla, H. S. Eds.; American Scientific Publishers. Vol:1, Chapter 1.
6. S. Gunes, H. Neugebauer, N. S. Sariciftci. Conjugated Polymer-Based Organic Solar Cells. *Chem. Rev.* (107)1324-1338, 2007.
7. R. H. Friend, R. W. Gymer, A. B. Holmes, J. H. Burroughes, R. N. Marks, C. Talian, D. D. C. Bradley, D. A. Dos Santos, J. L. Brédas, M. Lögdlund, W. R. Salaneck. Electroluminescence in Conjugated Polymers. *Nature* (397)121-128, 1999.

8. G. Horowitz., Organic Field-Effect Transistors. *Adv. Mat.* (10)365-377, 1998.
9. P. M. Beaujuge,J. R. Reynolds. Color Control in π-Conjugated Organic Polymers for Use in Electrochromic Devices. *Chem. Rev.* (110)268-320, 2010.
10. A. Heller. Electrical Wiring of Redox Enzymes. *Acc. Chem. Res.* (23)128-134, 1990.
11. L. Wen. Synthesis and Characterizations of Thieno [3,4-b] Pyrazine Based Low Band Gap Materials: Monomers, Oligomers and Polymers. 2008.
12. C. M. Mikulski, P. J. Russo,M. S. Saran, A. G. MacDiarmid, A. F. Garito,A. J. Heeger. *J. Am. Chem. Soc.* (97)6358-6363, 1975.
13. A. J. Heeger. Semiconducting and Metalic Polymers: The Fourth Generation of Polymeric Materials. *Angew Chem. Int Ed.* (40)2591-2611, 2001.
14. H. Shirakawa, E. J. Louis, A. G. MacDiarmid,C. K. Chiang, A. J. Heeger.*J. Chem. Soc. Chem. Commun.* 578-580, 1997.
15. T.A. Skotheim, R.L. Elsenbaumer, J. R. Reynolds (Eds.). Handbook of Conducting Polymers.*Marcel Dekker York.*1998.
16. S. J. Higgins. *Chem Soc. Rev.* (26)247, 1997.
17. Y. J. Cheng, S. H. Yang, C. S. Hsu. Synthesis of Conjugated Polymers for Organic Solar Cell Applications. *Chem. Rev.* (109)5868–5923, 2009.
18. E. E. Havinga, W. Hoeve,H. Wynberg. A New Class of Small Band Gap Organic Polymer Conductors. *Polymer Bulletin.*(29)119–126, 1992.
19. E. E. Havinga,W. Hoeve,H. Wynberg. Alternate Donor-Acceptor Small-Band-Gap Semiconducting Polymers; Polysquaraines and polycroconaines. *Synth. Met.*(55)299–306, 1993.
20. C. K.Chiang, Y. W.Park, A. J.Heeger, H.Shirakawa, E. J.Louis, A. G.MacDiarmid. *Phys. Rev. Lett.* (39)1098, 1977.
21. K. E. Ziemelis, A. T. Hussain, D. D. C. Bradley, R. H. Friend, J. Rilhe, G. Wegner. *Phys. Rev. Lett.* (66)2231, 1991.
22. C. K. Chiang, C. R. Fischer, Y. W. Park, A. J. Heeger, H.Shirakawa, E. J. Louisi, S. C. Gau, A. G. MacDiarmid, *Phys. Rev. Lett.* (39)1098, 1977.

23. C. K. Chiang, M. A. Druy, S.C. Gau, A. J. Heeger, E. J. Louis, A. G. MacDiarmid. Synthesis of Highly Conductive Films of Derivatives of Polyacetylene. *J. Am. Chem. Soc.* (100)1013-1015, 1978.
24. P. J. Nigrey, A. G. MacDiarmid, A. J. Heeger. Electrochemistry of Polyacetylene, $(CH)_x$: Electrochemical Doping of $(CH)_x$Films to the Metallic State. *J. Chem. Soc. Chem. Commun.*594, 1979.
25. E. Bundgaard, F. C. Krebs. Low Band Gap Polymers for Organic Photovoltaics*Solar Energy Materials & Solar Cells.* (91)954–985, 2007.
26. I. F. Perepichka, D. F. Perepichka, H. Meng, F. Wudl. Light-Emitting Polythiophenes. *Adv. Mater.* (17) 2281, 2005.
27. E. A. Meijere, F. Diederich, Metal Catalyzed Cross Coupling Reactions. *Wiley-VCH Weinheim.* (2), 2004.
28. J. K. Stille, *Angew. Chem. Int. Ed. Engl.* (25)508, 1986.
29. J. Roncali. Conjugated Poly(thiophenes): Synthesis, Functionalization and Applications. *Chem Rev.* (92)711, 1992.
30. G. Zotti, G. Schiavon, A. Berlin, G. Pagani. *Chem. Mater.* (5)430, 1993.
31. P. Audebert, P. Hapiot. Fast Electrochemical Studies of the Polymerization Mechanisms of Pyrroles and Thiophenes. Identification of the First Steps. Existence of π-Dimers in Solution. *Synthetic Metal.* (75)95, 1995.
32. R. Prakash,A. Somani, S. Radhakrishnan. Electrochromic Materials and Devices: Present and Future, *Materials Chemistry and Physics* (77)117–133, 2002.
33. P.M.S. Monk, R.J. Mortimer, D.R. Rosseinsky, Electrochromism: Fundamentals and Applications, *VCH, Weinheim*, 1995.
34. A. A. Avni, P. H. Aubert, B. C. Thompson, I. Schwendeman, C. L. Gaupp, J. Hwang, N. J. Pinto, D. B. Tanner, A. G. MacDiarmid, J. R. Reynolds.Multicolored Electrochromism in Polymers, *Chem. Mater.*2004, 16, 4401-4412.
35. M. A. Chad, L. D. Aubrey, J. R. Reynolds. Navigating the Color Palette of

Solution-Processable Electrochromic Polymers.*Chem. Mater.* (23)397–415, 2011.

36. Y. -J. Cheng, S. -H. Yang, C. -S. Hsu, Synthesis of Conjugated Polymers for Organic Solar Cell Applications, *Chem. Rev.,* 109) 5868-5923, 2009.
37. F. Marchioni, J. Yang, W. Walker, F.Wudl, A Low Band Gap Conjugated Polymer for Supercapacitor Devices, *J. Phys. Chem. B,* 110, 22202-22206, 2006.
38. A. Argun, A. Cirpan, J. R. Reynolds, The First Truly All-Polymer Electrochromic Devices, *Adv. Mater.*,15, 1338-1341, 2003.
39. G. Horowitz, Organic Field-Effect Transistors, *Adv. Mater.,* 10, 365-377, 1998.
40. A. P. Kulkarni , C. J. Tonzola , A. Babel , and S. A. Jenekhe, Electron transport materials for organic light-emitting diodes, *Chem. Mater.*,16, 4556-4573, 2004.
41. S. Demirci, F. B. Emre, F. Ekiz, F. Oğuzkaya, S. Timur, C. Tanyeli, L. Toppare,Functionalization of Poly-SNS-Anchored Carboxylic Acid with Lys and PAMAM: Surface Modifications for Biomolecule Immobilization/Stabilization and Bio-sensing Applications, *Analyst* 137, 4254-4261, 2012.
42. S. Gunes, H. Neugebauer, N. S. Sariciftci, Conjugated polymer-based organic solar cells, *Chem. Rev.* 107,1324-1338, 2007.
43. A. Cirpan, L. Ding, F.E. Karasz, Efficient Light Emitting Diodes from Polyfluorene Copolymer Blends, *Synth. Met.,* 150, 195-198, 2005.
44. P. M. Beaujuge, J. R. Reynolds, Color Control in π-Conjugated Organic Polymers for Use in Electrochromic Devices, *Chem. Rev.*, 268-320, 2010.
45. A. Balan, D. Baran, G. Gunbas, A. Durmus, F. Ozyurt, L. Toppare. One Polymer for all: Benzotriazole Containing Donor-Acceptor Ttype Polymer as a Multi-Purpose Material. *Chem. Commun*. 6768-6770, 2009.
46. G. Hızalan, A. Balan, D. Baran, L. Toppare. Spray Processable Ambipolar Benzotriazole Bearing Electrochromic Polymers with Multi-Colored and Transmissive States, *J. Mater. Chem.*,.(21)1804-1809, 2011.

47. M. F. G. Klein, F. M. Pasker, S. Kowarik, D. Landerer, M. Pfaff, M. Isen, D. Gerthsen, U. Lemmer, S. Höger, A. Colsmann. Carbazole–Phenylbenzotriazole Copolymers as Absorber Material in Organic Solar Cells. *Macromolecules* (46)3870-3878, 2013.
48. K. Li, Z. Li, K. Feng, X. Xu, L. Wang, Q. Peng. Development of Large Band-Gap Conjugated Copolymers for Efficient Regular Single and Tandem Organic Solar Cells. *J. Am. Chem. Soc.* (135)13549-13557, 2013.
49. B. Liu, X. Chen, Y. Zou, L. Xiao, X.Xu, Y. He, L. Li, Y. Li.Benzo[1,2-b:4,5-b′]difuran-Based Donor–Acceptor Copolymers for Polymer Solar Cells, *Macromolecules* (45)6898, 2012.
50. J. Min, Z. G. Zhang, S. Zhang. Conjugated Side-Chain-Isolated D–A Copolymers Based on Benzo[1,2-b:4,5-b′]dithiophene-alt-dithienylbenzotriazole: Synthesis and Photovoltaic Properties. *Chem. Mater.* (24)3247-3254, 2012.
51. J. Min, Z.G. Zhang, S. Zhang, M. Zhang, J. Zhang, Y. Li. Synthesis and Photovoltaic Properties of D–A Copolymers Based on Dithienosilole and Benzotriazole. *Macromolecules* (44)7632-7638, 2011.
52. S. C. Price, A. C. Stuar, L. Yang, H. Zhou, W. You. Fluorine Substituted Conjugated Polymer of Medium Band Gap Yields 7% Efficiency in Polymer-Fullerene Solar Cells. *J. Am. Chem. Soc.* (133)4625-4631, 2011.
53. D. Kotowski, S. Luzzati, G. Bianchi, A. Calabrese, A. Pellegrino, R. Po, G. Schimperna, A. Tacca. Double Acceptor D–A CopolymersContaining Benzotriazole and Benzothiadiazole Units: Chemical Tailoring Towards Efficient Photovoltaic Properties. *J. Mater. Chem. A* (1)10736-11080, 2013.
54. B. Liu, X. Chen, Y. He, Y. Li, X. Xu, L. Xiao, L. Li, Y. Zou. New Alkylthienyl Substituted Benzo[1,2-b:4,5-b′]dithiophene-Based Polymers for High Performance Solar Cells. *J. Mater. Chem. A* (1)570-577, 2013.
55. A. Balan, D. Baran, L. Toppare. Processable Donor–Acceptor type electrochromes Switching BetweenMulticolored and Highly Transmissive

States Towards Single Component RGB-based Display Device. *J. Mater. Chem.* (20)9861-9866, 2010.

56. N. A. Unlu, T. K. Deniz, M. Sendur, A. Cirpan. Effect Of Dithienopyrrole Unit On Electrochromic And Optical Properties Of Benzotriazole Based Conjugated Polymers, *Macromol. Chem. Phys.* (213)1885-1891, 2012.
57. S. C. Cevher, N. A. Unlu, A. C. Ozelcaglayan, D. H. Apaydin, Y. A. Udum, L. Toppare,A. Cirpan. Fused Structures in the Polymer Backbone to Investigate the Photovoltaic and Electrochromic Properties of Donor-Acceptor Type Conjugated Polymers. *Polym. Chem.* (51)1933-1941, 2013.
58. A. Patra, M. Bendikov. Polyselenophenes. *J. Mater. Chem.* (20)422-433, 2010
59. H. Y. Chen, C. S. Yeh, C. T. Chen. Comparison of Thiophene- and Selenophene-Bridged Donor–Acceptor Low Band-Gap Copolymers Used in Bulk-Heterojunction Organic Photovoltaics. *J. Mater. Chem.* (22)21549-21559, 2012.
60. M. Shahid, T. McCarthy-Ward, J. Labram, S. Rossbauer, E. B. Domingo, S. E. Watkins, N. Stingelin, T. D. Anthopoulos, M. Heeney. Low Band Gap Selenophene–Diketopyrrolopyrrole Polymers Exhibiting High and Balanced Ambipolar Performance in Bottom-Gate Transistors. *Chem. Sci*. (3)181-185, 2012.
61. A. A. B. Alghamdi, D. C. Watters, H. Yi, S. Al-Faifi, M. S. Almeataq, D. Coles, J. Kingsley, D. G. Lidzey, A. Iraqi. Selenophene vs. Thiophene in Benzothiadiazole-Based Low Energy Gap Donor–Acceptor Polymers for Photovoltaic Applications. *J. Mater. Chem. A* (1)5165-5171, 2013.
62. J. J. Intemann, K. Yao, H. L. Yip, Y. X. Li, P. W. Liang, F. Z. Ding, X. Li, A. K. Y. Jen. Molecular Weight Effect on the Absorption, Charge Carrier Mobility, and Photovoltaic Performance of an Indacenodiselenophene-Based Ladder-Type Polymer. *Chem. Mater.* (25)3188-3195, 2013.

63. B. Kim, H. R. Yeom, M. H. Yun, J. Y. Kim, C. Yang. A Selenophene Analogue of PCDTBT: Selective Fine-Tuning of LUMO to Lower of the Bandgap for Efficient Polymer Solar Cells. *Macromolecules* (45)8658-8664, 2012 .
64. D. H. Wang, A. Pron, M. Leclerc, A. J. Heeger.Additive-Free Bulk-Heterojuction Solar Cells with Enhanced Power Conversion Efficiency, Comprising a Newly Designed Selenophene-Thienopyrrolodione Copolymer. *Adv. Funct. Mater.* (23)1297-1304, 2013.
65. L. Dou, W. Chang, J. Gao, C. C. Chen, J. You, Y. Yang. A Selenium-Substituted Low-Bandgap Polymer with Versatile Photovoltaic Applications. *Adv. Mater.* (25)825-831, 2013.
66. S. C. Cevher, N. A. Unlu, A. C. Ozelcaglayan, D. H. Apaydin, Y. A. Udum, L. Toppare, A. Cirpan. Fused Structures in the Polymer Backbone to Investigate the Photovoltaic and Electrochromic Properties of Donor-Acceptor Type Conjugated Polymers. *Polym. Chem.* (51)1933-1941, 2013.
67. S. S. Zhu, T. M. Swager. Conducting Polymetallorotaxanes: Metal Ion Mediated Enhancements in Conductivity and Charge Localization. J. Am. *Chem. Soc.* (119)12568-12577, 1997.
68. N. Sumi, H. Nakanishi, S. Ueno, K. Takimiya, Y. Aso, T. Otsubo. Synthesis and Properties of a Series of the Longest Oligothiophenes up to the 48-mer. *Bull. Chem. Soc. Jpn.* (74)979-988, 2001.
69. Y. J. Hwang, N. M. Murari, S. A. Jenekhe. New n-type Polymer Semiconductors Based on Naphthalene Diimide and Selenophene Derivatives for Organic Field-Effect Transistors. *Polym. Chem*. (4)3187-3195, 2013.
70. A. Argun, P. H. Aubert, B. C. Thompson, I. Schwendeman, C. L. Gaupp, J. Hwang, N. J. Pinto, D. B. Tanner, A. G. MacDiarmid, J. R. Reynolds. Multicolored Electrochromism in Polymers: Structures and Devices, *Chem. Mater.* (16)4401-4412, 2004.

APPENDIX A

NMR DATA

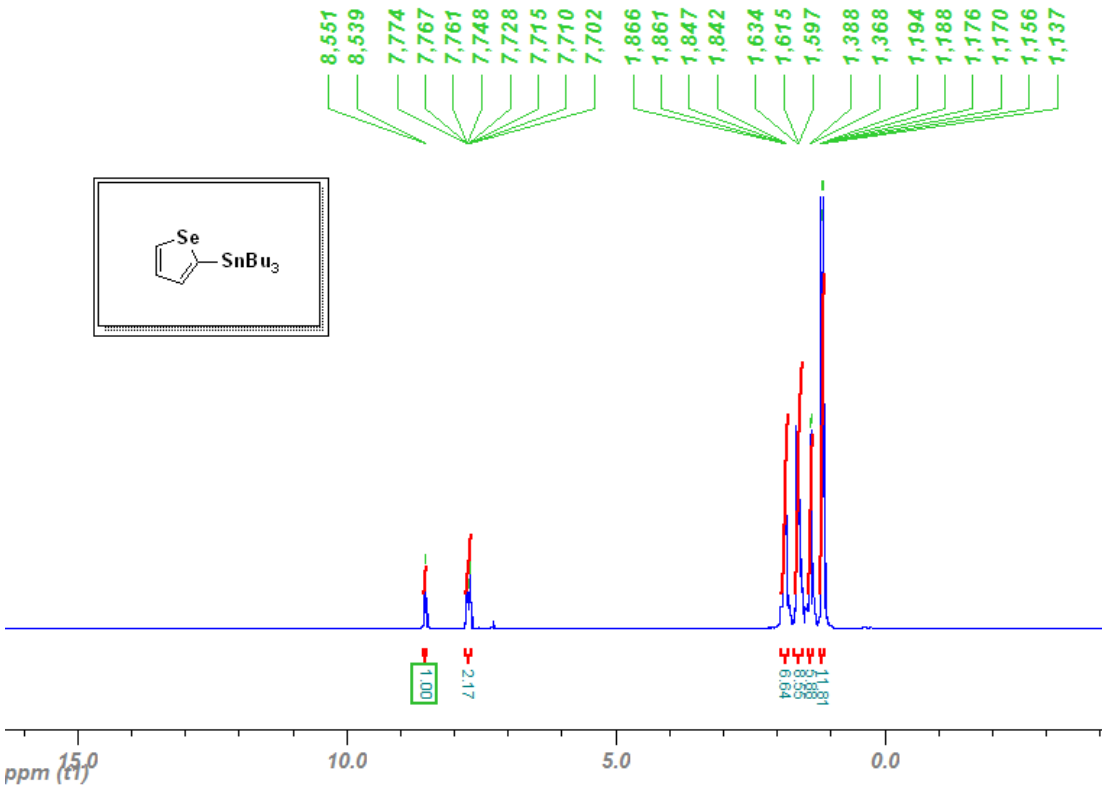

Figure 37. ^{1}H NMR of Tributyl(selenophen-2-yl)stannane

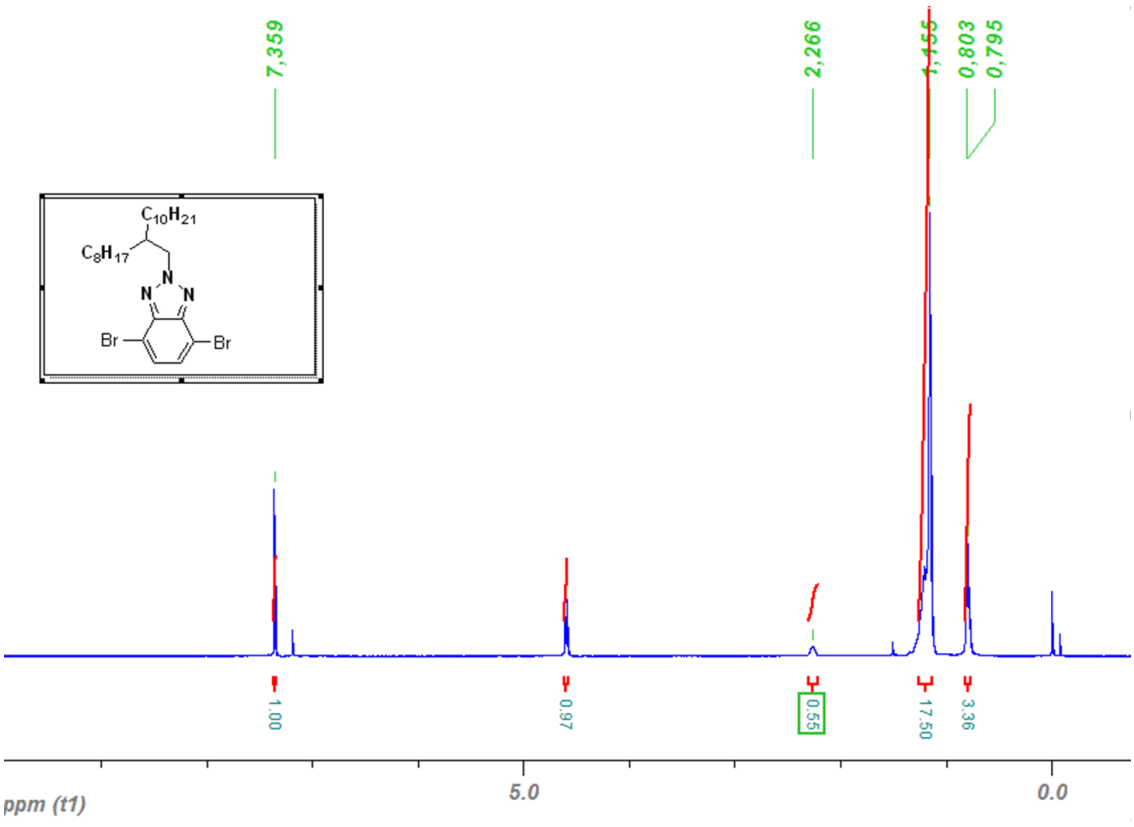

Figure 38. ^{1}H NMR of 4,7-dibromo-2-(2-octyldodecyl)-2H-benzo[d][1,2,3]triazole

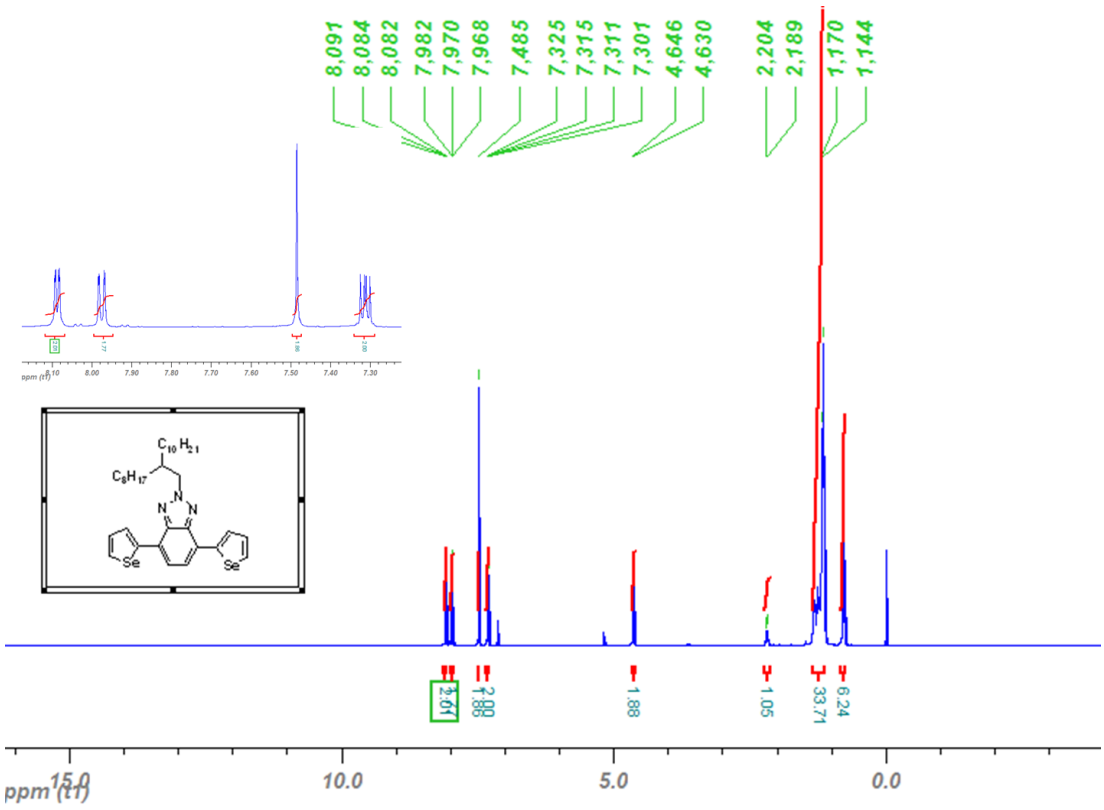

Figure 39. ^{1}H NMR of 2-(2-octyldodecyl)-4,7-di(selenophen-2-yl)-2H-benzo[d][1,2,3]triazole

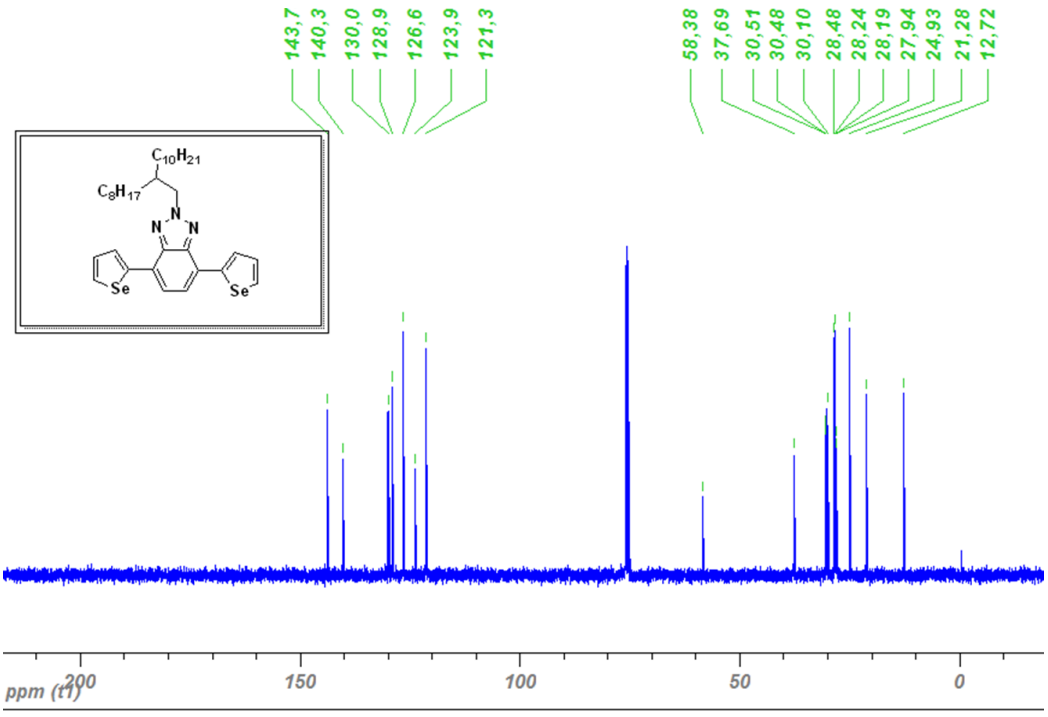

Figure 40. ^{13}C NMR of 2-(2-octyldodecyl)-4,7-di(selenophen-2-yl)-2H-benzo[d][1,2,3]triazole

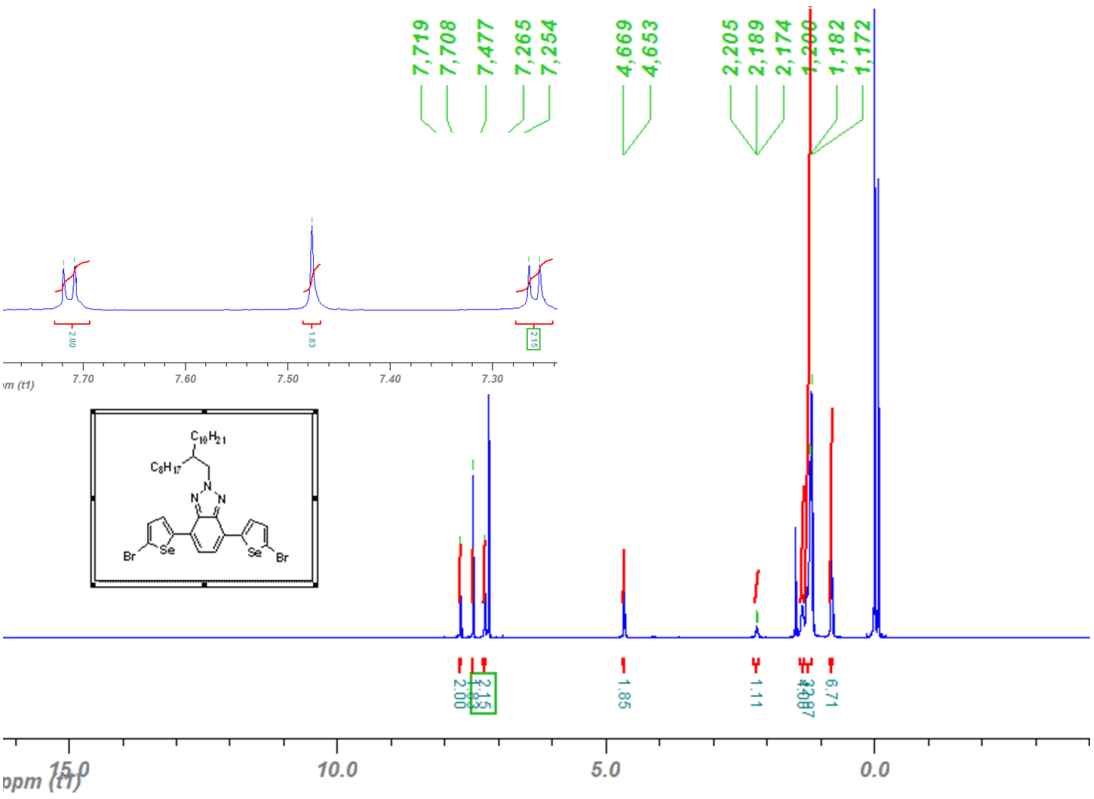

Figure 41.[1]H NMR of 4,7-bis(5-bromoselenophen-2-yl)-2-(2-octyldodecyl)-2H-benzo[d][1,2,3]triazole

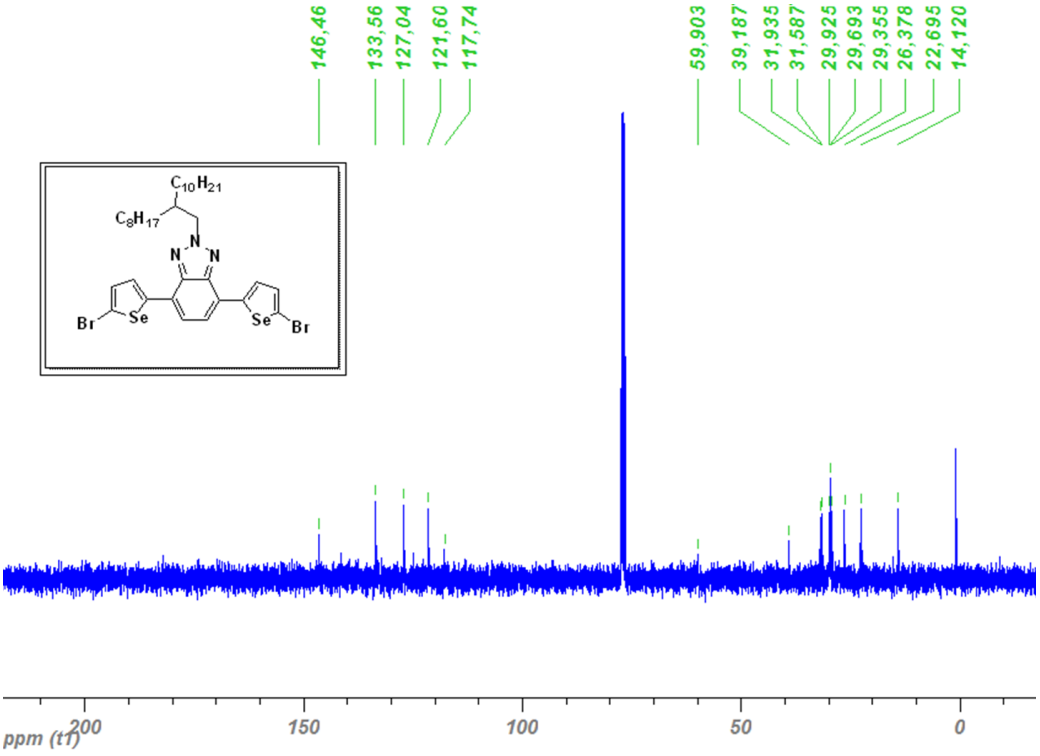

Figure 42.[13]C NMR of 4,7-bis(5-bromoselenophen-2-yl)-2-(2-octyldodecyl)-2H-benzo[d][1,2,3]triazole

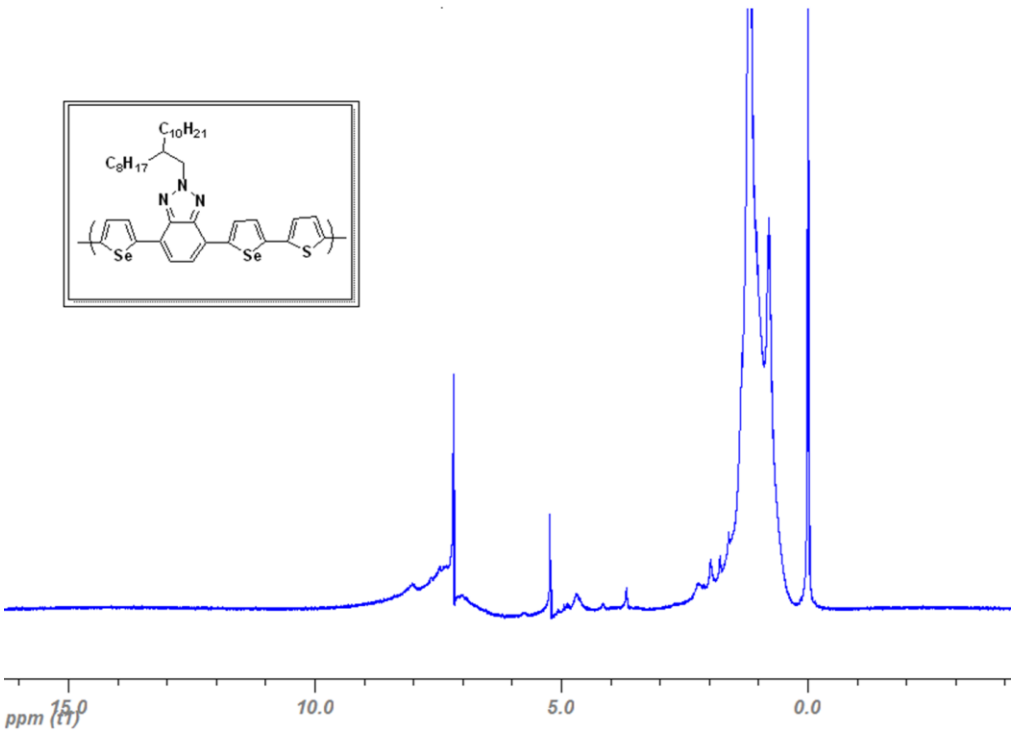

Figure 43.^{1}H NMR of **P-SBTTh**

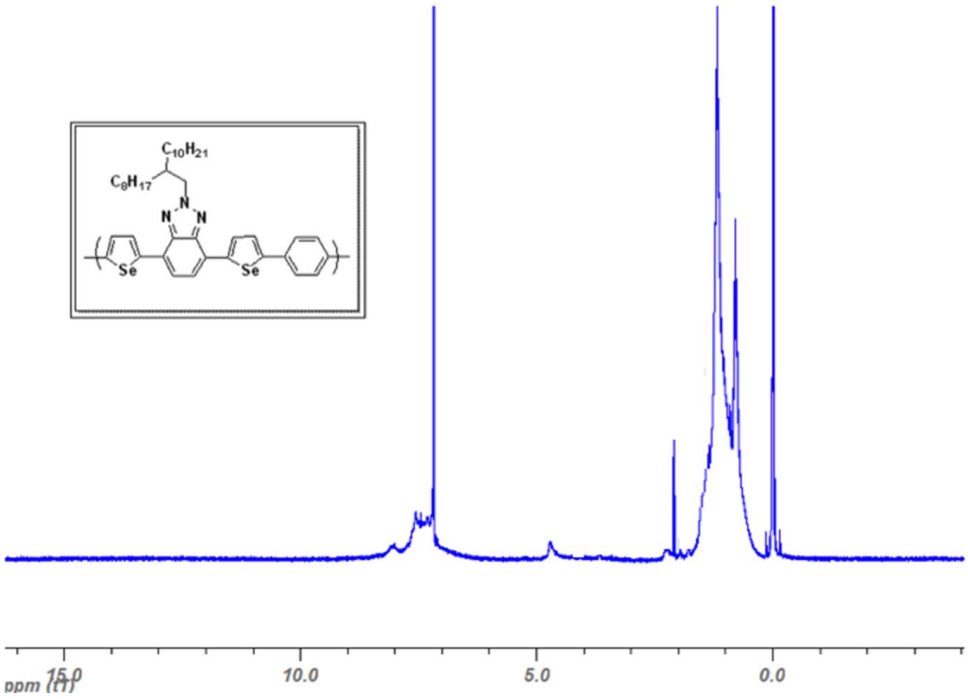

Figure 44.[1]H NMR of **P-SBTPh**